UAB

Treball de Fi de Grau

Grau en Enginyeria de Sistemes de Telecomunicació

Dual-Frequency techniques for GNSS receivers.

Joan Miguel Bernabeu Frias

Director: Daniel Egea Roca

Departament de Telecomunicació i Enginyeria de Sistemes

Universitat Autònoma de Barcelona

Bellaterra, Juny 17, 2019

Abstract

This thesis studies the implications of using signal measurements from different frequency bands in satellite navigation. With this purpose, several tests will be carried out comparing a set of signal configurations, and combining its measurements following different techniques to mitigate ionosphere errors. In the first place, GPS L1/L5 and Galileo E1/E5 signals will be analysed to later compare their corresponding results when used for positioning. The latter will be useful to determine which signals provide receivers with more accurate estimates of their position. In the second place, methods to compensate ionosphere errors will be presented and tested. In these tests, special emphasis will be made in the case of the GPS constellation, with the aim of increasing its correction factor as it counts with more limitations to compensate ionosphere effects than the Galileo GNSS. To perform these tests, a positioning algorithm is developed in MATLAB, which takes as input parameters the observables contained in a RINEX file from a selected reference station.

The present thesis contains the work carried out to characterise and mitigate ionosphere effects in the application presented by students from Universitat Autònoma de Barcelona (UAB) to the *'Galileo App competition'* contest organized by the European Space Agency (ESA), which took place in April 2019.

Agradecimientos

En primer lugar, quiero mostrar mi agradecimiento al Dr. Daniel Egea Roca, por todo lo que he aprendido de él y por el tiempo y dedicación que ha empleado en mí.
En segundo lugar, quisiera dar las gracias a mi familia y a mis amigos, por apoyarme incluso estando a kilómetros de distancia.
Por último, agradecer a mis compañeros de trabajo en GMV por atender a la larga lista de dudas que cada día les he ido preguntando.

Resum

Aquest memòria estudia les implicacions d'utilitzar mesures de diferents bandes de freqüències per a la navegació per satèl·lit. Amb aquest propòsit, diversos tests seran portats a terme comparant els diferents senyals i utilitzant les seves mesures seguint una sèrie de tècniques per a mitigar els efectes de la ionosfera. En primer lloc, les senyals L1/L5 de GPS i E1/E5 de Galileo seran analitzades per a després comparar els seus respectius resultats quan son utilitzades per al posicionament. Aquests últims, seran d'utilitat per a determinar quines proporcionen als receptors GNSS amb mesures de posició més precises. En segon lloc, diversos mètodes per a compensar errors ionosfèrics seran testejats. En aquests, es posarà especial èmfasi en el cas de GPS, amb l'objectiu de millorar el seu factor de correcció, degut a que aquest presenta més limitacions de cara a compensar errors de la ionosfera en comparació amb Galileo. Per a la realització d'aquests tests, un algoritme de posicionament serà portat a terme a MATLAB, el qual prendrà com a paràmetres d'entrada valors continguts a un arxiu RINEX, d'una estació de referència prèviament seleccionada.

La present memòria conté el treball portat a terme per a caracteritzar i mitigar errors ionosfèrics a l'aplicació presentada per la Universitat Autònoma de Barcelona per al concurs *'Galileo App Competition'* organitzat per l'Agència Espacial Europea (ESA), el qual va tenir lloc a l'Abril de 2019.

Resumen

Esta memoria estudia las implicaciones de usar medidas de diferentes bandas de frecuencia para la navegación por satélite. Con este propósito, varios tests serán llevados a cabo comparando las diferentes señales y usando sus medidas siguiendo diferentes técnicas para mitigar los efectos de la ionosfera. En primer lugar, las señales L1/L5 de GPS y E1/E5 de Galileo serán analizadas para luego comparar sus respectivos resultados cuando son usadas para el posicionamiento. Estos últimos serán útiles para determinar que señales proporcionan a los receptores GNSS con medidas de posición más precisas. En segundo lugar, varios métodos para compensar errores ionosféricos serán propuestos y testeados. En estos, se pondrá especial énfasis en el caso de GPS, con el objetivo de mejorar su factor de corrección, debido a que este presenta más limitaciones para compensar errores de ionosfera en comparación con Galileo. Para realizar estos tests, un alogritmo de posicionamiento será llevado a cabo en MATLAB, el cual tomara como parámetros de entrada valores contenidos en un archivo RINEX, de una estación de referencia seleccionada.

La presente memoria contiene el trabajo llevado a cabo para caracterizar y mitigar errores ionosféricos en la aplicación presentada por estudiantes de la Universidad Autónoma de Barcelona (UAB) para el concurso *'Galileo App Competition'* organizado por la Agencia Espacial Europea (ESA), el cual tuvo lugar en Abril de 2019.

Contents

List of Figures

List of Tables

Glossary

Terms and definitions:

- **Signal measurement:** Signal measurements are the user-to-satellite ranges that receivers compute from satellite signals.
- **RMSE:** This metric has been used profusely in this document, it makes reference to the root-mean-squared error measured using the three Cartesian coordinates (X,Y,Z) from a positioning solution relative to the reference position.
- **PRN:** This acronym stands for Pseudo-random-noise code, and it is often used in this document to identify satellites within a constellation as they all count with different and known codes.
- **Epoch:** A time epoch defines a time stamp within the time reference selected, e.g. GPS or Galileo time references.
- **LoS:** Line-of-Sight refers to the imaginary line traced between the receiver and the satellite in question.
- **CN0:** Carrier-to-Noise ratio is the signal-to-noise ratio of a modulated signal.

Acronyms:

- **GNSS:** Global Navigation Satellite System
- **GPS:** Global Positioning System
- **GAL:** Galileo
- **PVT:** Position-Velocity-time

- **CDF:** Cumulative Distribution Function
- **BW:** Bandwidth
- **DSSS:** Direct-Sequence Spread Spectrum
- **CDMA:** Code-Division Multiple Access
- **CIRS:** Conventional Inertial Reference System
- **CTRS:** Conventional Terrestrial Reference System
- **WGS:** World Geodetic System

Chapter 1

Introduction

Global Navigation Satellite Systems (GNSS) count with complex and ever-developing technologies whose aim is to provide receivers with accurate and low-demanding navigation services all around the world. The former, thanks to the ever-cheapening receiver's equipment, have been able to be deployed and established globally, to the extend nowadays it constitutes a daily-use tool for countless applications in many different environments, amongst which are either the military and the user sectors. It is curious how easy it is nowadays for anybody to access to basic navigation services in contrast to the complex processes which are needed to offer them.
Many different applications are beneficiaries of navigation facilities with more or less demanding requirements (see [1]). All of them have in common that the better the positioning accuracy, the more they will embrace and rely on satellite navigation services. To pursue the goal, constant research is required for either designing new system features and mitigate current malfunctions and/or error sources.

1.1 Motivation and Objectives

There are several ways to improve navigation accuracy and performance. On the one side, newer signals or communication techniques could be studied and put into practice in order to optimise or relax certain requirements. On the other side, current error sources could be mitigated so that actual positioning systems had tools to avoid being incurred into error due to internal components or external threats.
Error sources are diverse, they can be related to component imperfections in either the

space, the control and the user segment, and also to outer effects such as errors due to obstacles, atmosphere effects etc. However, one of the most considerable error sources is the ionosphere layer (see [2]), as it substantially delays satellite radio-signals, incurring receiver measurements in error. Its effects can be compensated by using GNSS broadcast models or by combining measurements received from the same satellite in two different frequencies (DF measurements).
Until not so long ago, only professional receivers could access to DF measurements so as to navigate and develop efficient correction techniques. Nonetheless, with the GPS modernisation plan started at 2010 [3] and the progressively deployment of Galileo constellation [4], more signals from different frequency bands are being offered to non-professional receivers. Besides, in 2016 Android OS mobile phones received and update that made accessible GNSS raw measurements [5], which in addition to the increasing mobile phone receivers compatibility with L5/E5 signals, opened the way to users to access DF measurements.
In conclusion, the latter are becoming more and more present not only in dedicated GNSS receivers but also in mass-market devices, which motivates the study of their characteristics and effects in navigation. For this, this research will analyse and test the different GPS and Galileo signals located in L1/E1 and L5/E5 frequency bands, and finally evaluate the benefits obtained from DF measurements to mitigate ionosphere errors.
Based on the above considerations, the goals of this thesis can be summarised in the following list:

1. **Analyse PVT capabilities for signals at different frequency bands.**

2. **Analyse Ionosphere corrections:**

   (a) Model Based (i.e. Klobuchar)

   (b) DF Measurements.

As aforementioned, this research has gone hand to hand with a contest organised by the *European Space Agency* (ESA) named *Galileo App competition* [6], started at September 2018 and ended at April 2019. Between the competitors implied, there was *INARI team* from Universitat Autònoma de Barcelona (UAB), which received **two prizes** for their work. The main goal of this contest was to develop a Smartphone Application which used mobile phone DF measurements to navigate and to perform corrections.

1.2 Document structure

The contents of this document will be divided in three parts, constituting a total of three chapters and the conclusions.

Chapter 2, will give context of GNSS navigation basics, introducing the reader into the well known positioning equations, in the most comprehensive and understandable manner possible. This part will lead to introduce the main topic of the second part of the document, which concerns the use of DF measurements for positioning and to mitigate ionosphere effects on GPS and Galileo signals.

That being said, chapter 3 is again divided in two parts. The first one will analyse GPS and Galileo available signals so as to shed light to their specifications and pros and cons. Part two addresses ionosphere effects in detail. The latter will explain and characterise them to finally present the means to mitigate them from a theoretical perspective.

Chapter 4 will gather a set of tests aimed to prove, on the one hand, which signals are better for navigation, and on the other hand, which correction techniques are better for subtracting ionosphere errors from measurements.
Finally, conclusions extracted will be summed up in Chapter 5 where, in addition, further lines of research will be pointed out.

Chapter 2

GNSS Positioning

2.1 Brief history overview of GNSSs services

The fact of placing electronic devices in the sky, in such a way that they serve as a tool for geolocation and timing has been a remarkable achievement in history of humanity. As soon as satellite navigation systems became a reality, they altered the course of many other technologies and sectors either military and civil. Although the first GNSS, which was U.S. Global Positioning System (1973) and mostly thought for military purposes, with the past of the time it also started to become of great interest in many other areas to the extent that nowadays, civilian applications constitute one of the most active and frequently used branch of GNSSs. Multiple sectors make use of satellite navigation, such as transport, aviation, basic user location just to mention a few.
Before GNSSs, the most well established navigation systems were ground-based and made use of radio-signals, to perform what it is known as hyperbolic navigation, e.g. Long Range Radio Navigation (LORAN) and Decca Navigator System. This class of navigation systems were used by the U.S. during World War II and used infrastructure located at strategic points to transmit synchronous signals to receivers within their range of operation.

The principle, behind this technique basically consisted on defining a serial of hyperbolas over a determinate area, taking as the foci two base-stations (BS) who played the role of transmitters. Considering that the summation of the distance from both focis to any point within the hyperbola radius remains constant, and that the signals' travel time are known, i.e., the transmission time is known, it is possible to locate the

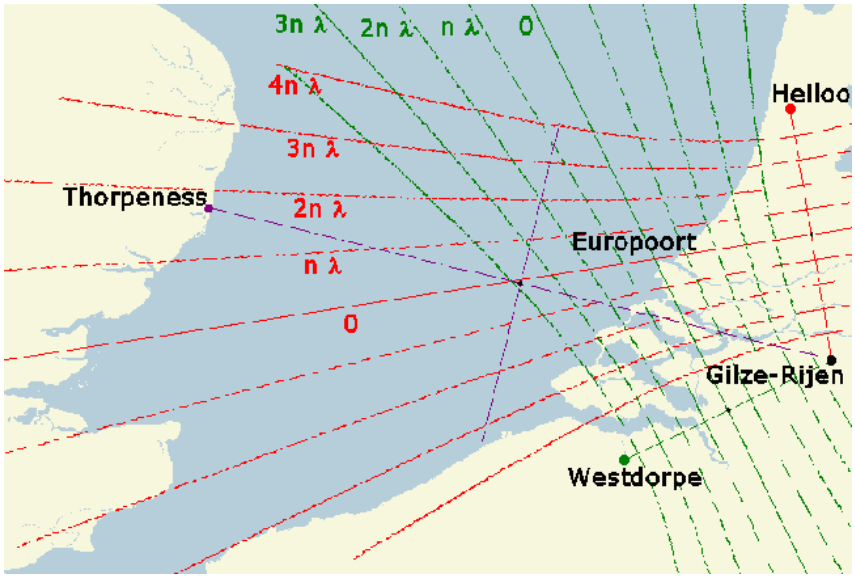

Figure 2.1: LORAN hyperbolic positioning system operating in England.

receiver within a concrete hyperbola. However, in order to know in which concrete point is it located, an additional hyperbola is required, whose new radius cuts the previous one. To compute two pairs of hyperbola focis, and obtain a concrete point, only three transmitters are needed if one of them is reused to form two pairs. This principle is graphically described in figure 2.1 from [7], where it is displayed a LORAN system in the region of England. More dedicated information about hyperbolic navigation can be found in [7] and [8](ch.1.2.2).

Although these techniques proved to be effective in certain scenarios, at the same time, had strong limitations in terms of scalability and availability:

- **Scalability**: The coverage area defines the zone in which receivers are able to make use of the positioning system. In this case, to increase the operation coverage, new BS need to be set up, but it is obvious that there are political issues over countries that prevents an unlimited deployment.

- **Availability:** The signal path from the BS to the receiver is more or less straight and relatively parallel to the earth's surface, which means that there are many obstacles that compromises the system availability in scenarios that are not geographically plain. Even though there are techniques that use the ionosphere layer to reflect BS signals to transmit information over the horizon, these are also limited by obstacles and only work in specific conditions (see [9] for more information)

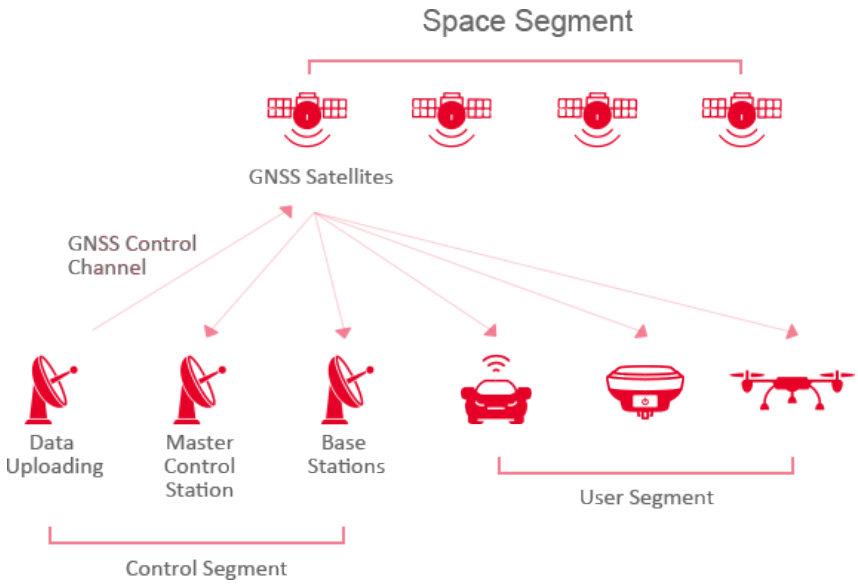

Figure 2.2: GNSS segments

These system limitations, together with the launch of the first artificial satellite by the Soviet Union (Sputnik-1 [10], 1957) motivated the study and deployment of a new Satellite positioning system, which could locate receivers all around the world and overcome the previous mentioned ground-based system limitations. With this, the primary world powers such as U.S. and the old Soviet Union started to build their own satellite constellations and ever since their launching have been under development with periodical improvements and monitoring. Other powers joined this particular space race later on, such as Europe with Galileo [11] and China with Beidou [12].

The basic function of a navigation satellite is to transmit basic information containing key parameters which the receiver will use in order to compute certain measurements, that are required in the positioning algorithm. A GNSS is a passive service for its users, however, it requires constant control over its satellites so as to prevent and avoid anomalies and keep the system performing well.
GNSS are classically divided into three different parts (see figure 2.2 from Tersus); the space segment, the control segment and the user segment. These segments are described next:

- **Space Segment:** Comprises the Satellite constellation which transmits radio signals to users.

- **Control segment:** Consists of worldwide monitor and control stations, aimed to

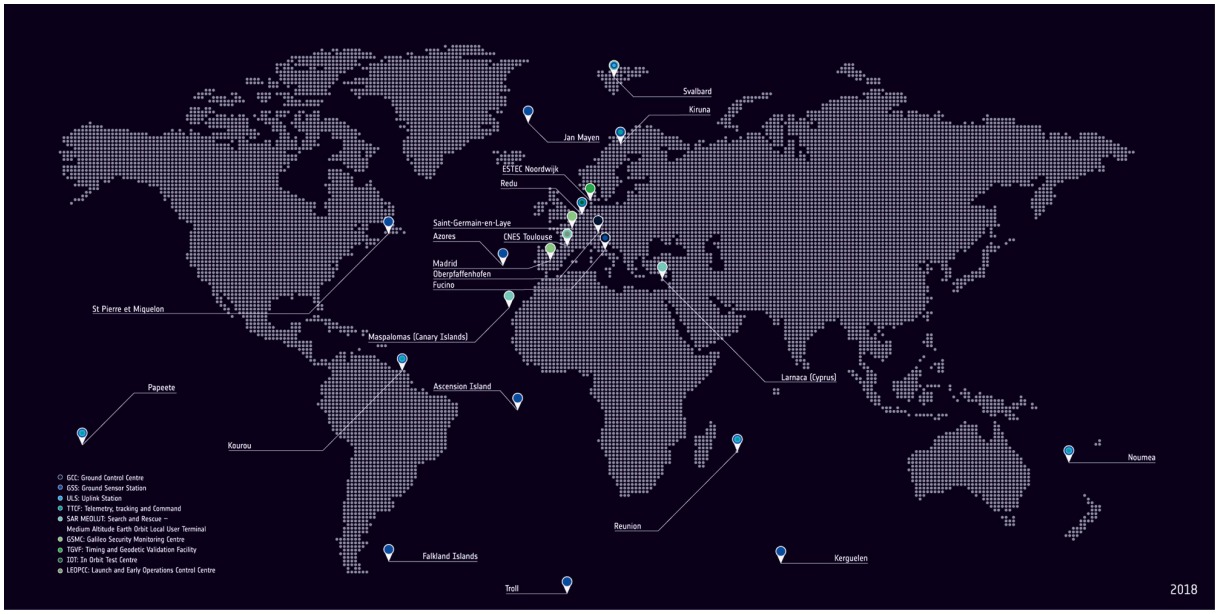

Figure 2.3: Galileo's control segment stations around the world.

maintain satellites in their corresponding orbits through periodical corrections, to adjust satellite clocks and to upload updated navigational data. This segment is generally formed by a master control station and various monitoring sites. In figure 2.3 from [13], all Galileo's control segment stations are displayed.

- **User Segment:** Consists of receivers equipment, which sense satellite's signals and use the information obtained to calculate their position, velocity and time (PVT).

For further information, see [14].

2.2 The GPS and the Galileo systems

On the one hand, the GPS project took its firsts steps thanks to the U.S. Department of Defence in the mid 1960's and was fully operational in 1993. Today it is a multi-use radio-navigation system owned by the U.S. Government and operated by the United States Air Force. Although in the beginning it counted with a fleet of 24 satellites with nearly global coverage, nowadays this number has increased to 31 at the reporting date, located approximately at 20,180 km from Earth's surface. From 1990 until 2000, GPS performance was degraded on purpose as the U.S. government realised that even amateur users could reach surprisingly good position accuracy through signal processing techniques, which constitute a thread. This intentional degradation was called selective

availability (SA) [15] , and induced errors in the order of 50 meters horizontally and 100 vertically.

On the other hand, Galileo is the GNSS created by the E.U. through the European GNSS Space Agency (GSA) in 2003 officially. It was initially designed to inter-operate with other satellite constellations such as GPS and Glonass [16]. Its name comes from the historical Italian astronomer Galileo Galilei, and counts with 30 satellites in orbit at around 23.000 km from the Earth's surface.
The main objective of the E.U. with the Galileo project was to own an independent GNSS controlled by its country members which guaranteed positioning no matter the political circumstances. As the GPS control is held by the U.E., its service can denied in any region at any moment, or even errors in measurements can be induced, degrading selectively the system performance as above mentioned.
Although Galileo's initial services became available on 15 December 2016, the system completion is scheduled for 2020 according to [11]. As Galileo's satellites are relatively new, they include more advanced equipment and use more sophisticated signals. However, this does not mean that it always performs better than other constellations which have been operating for longer and count with much more expertise.

2.2.1 Services

Although GPS and Galileo are able to inter-operate to improve satellite availability and positioning accuracy, they follow distinct approaches in terms of signalling and coding. Both signal plans count with more than one signal per band, with different characteristics in order to be able to offer multiple positioning services. As it is demonstrated later in chapter 5, different positioning results will be obtained depending on the signals considered in the positioning algorithm. For this, each constellation offers various services using different signal combinations. These are noted and explained below for either GPS or Galileo.

GPS for its part, offers the Precise Positioning Service (PPS) and the Standard Positioning service (SPS):

- **Standard Positioning Service:** It offers positioning services with standard accuracy by means of the non-encrypted signals. However, as it has been mentioned

before, standard positioning service can be intentionally degraded or denied at any time by the U.S. control segment.

- **Precise Positioning Service:** It is only available to authorised users, and combines either civilian and the encrypted signals to improve accuracy, signal robustness and integrity. It also counts with anti-spoofing techniques.

In the case of the Galileo system, it offers the Open Service (OS), the High Accuracy Service (HAS), the Public Regulated Service (PRS) and the Search and Rescue Service (SRS):

- **Open Service:** It is the equivalent to the standard service on GPS, that is, it offers positioning with a standard accuracy with the non-encrypted signals.
- **High Accuracy Service:** This service is set to offer not only an enhanced accuracy but also authentication services, which means that signals used contain protection layers to avoid either intentional and unintentional interference (Jamming and/or Spoofing).
- **Public Regulated Service:** The PRS is, again, the equivalent to the GPS's PPS, as it uses encrypted signals and is only available for authorised users. The services it offers are enhanced resilience and robustness.
- **Rescue Service:** This innovative service aims to locate and help people in the case of an emergency by helping operators to respond to distress signals faster and more efficiently. It is designed to be available globally.

In tables 3.1 and 3.2, the different signal configurations used in this research have been summed up. As it has been stated above, there are more available options, however, some of them are not accessible or were not considered. This is explained in section 2.4; basically L1-L5 and E1-E5 combinations were selected for comparative purposes and because proved to be better for our objectives.

2.2.2 Spreading modulation and access technique

As each of the parameters from tables 3.1 and 3.2 before mentioned are relevant and have great impact in the overall system performance, it is worthy to describe some of

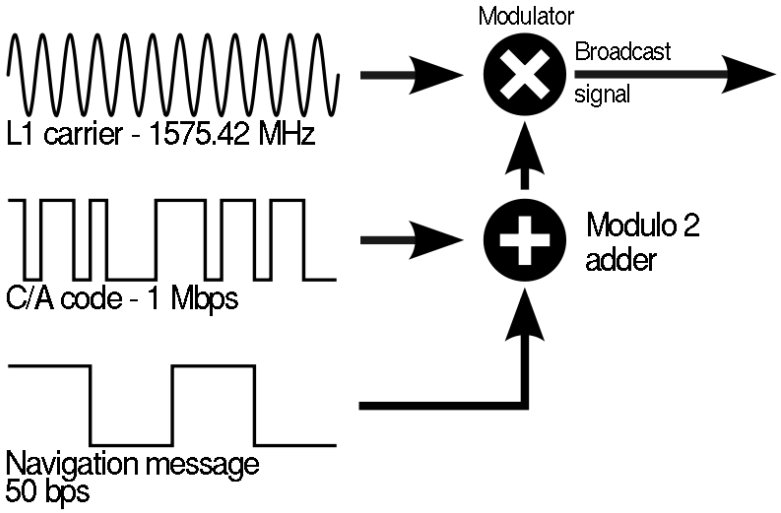

Figure 2.4: Block diagram of GPS C/A codes.

them in more detail. This subsection is aimed at giving an overview of the concepts of Spreading modulation and access technique.

In the first place, a channel access method allows multiple devices connected to the same transmission medium to transmit over it, sharing its capacity. That being said, as satellites transmit in the same frequency bands and are not time-multiplexed, an appropriate multiple access technique is required. As navigation satellite signal power levels are very low and are affected by Doppler effects, the access technique which fits best the system is Code-Division Multiple access (CDMA) [17] which constitutes a practical use of what is know as Direct-Sequence Spreading Spectrum (DSSS) [18].
DSSS is a spread spectrum modulation technique used to reduce overall signal interference. When satellite navigation messages are modulated using DSSS, they are multiplied by a bit sequence of much shorter duration, or equivalently, much larger bandwidth. In result, the output signals spread over the spectrum to the extend their power spectral density remains below that of the noise level, which is distributed equally through all frequencies with a certain variance. In consequence, all satellite signals are overlapped among each other in the same spectrum and with a modest power level. The block diagram of the modulation process for the case of GPS is showed in figure 2.7, and was obtained from [8].

With this, some questions about how receivers are able to obtain and differentiate each satellite signals may arise. The answer to this questions is provided by the CDMA technique. In a GNSS, CDMA is in charge of multiplexing different satellites which are using DNSS to access the medium. The basic principle behind this technique consists in

providing each satellite with a different spreading code, which is also known by receivers. Then, when the receiver wishes to obtain a specific satellite's navigation data from the signal received, which is in fact a mix of several signals, it replicates the corresponding satellite spreading code and performs an operation to recover the signal with much better power levels.
This operation is in fact a correlation, and in order to obtain the expected results, the spreading codes from each satellites have to meet with the following requirements:

1. Auto-Correlation ≈ 1
2. Cross-Correlation ≈ 0

This way, when the receiver correlates all the input signals with the local replica, for all correlations in which the two signals are different the result obtained will be near zero. In contrast, when the receiver correlates a pair of identical signals, the result obtained is near to one in the adequate code shift.
The codes used in GNSS which meet this requirements are a family of Gold codes and are called Pseudo-random noise codes or PRN, because they have a spectrum similar to a random sequence but are generated deterministically using shift registers. In the GPS constellation, satellites are often referred to as '$PRN\ X$', being 'X' the number of the corresponding PRN code used by that concrete satellite. For more information regarding the properties or the construction of these codes, the user is referred to [19].

2.3 GNSS Coordinates, time and orbits

In the process receivers follow to compute their position, it is mandatory to have an estimate of the receiver's a priori position and to know as precisely as possible satellite locations. With these two measurements, the receiver will compute a distance. In order to be able to perform such operations, these positions should be expressed in a common coordinate system. However, satellite's and receiver's positions have different requirements, for this reason, two reference systems are used for each other.
On the one side, the position of a user is expressed in a coordinate system that is fixed to the earth and moves with it. If this reference system did not move in accordance to the earth's rotation, the coordinates which locate users would be constantly changing even though the user is steady due to the Earth's spin. This reference system is called

Conventional Terrestrial Reference System (CTRS).
On the other side, the above coordinate system is not suited to the analysis of satellite motion, as satellites do not move in accordance to the Earth's spin. Satellite's motion is governed by the equations of motion, which require to be expressed in an inertial reference system. The latter, is called Conventional Interial Reference System (CIRS), and is a coordinate system which is defined fixed in space with respect to celestial parameters.

As aforementioned, in order to perform distance measurements, satellite's and receiver's position needs to be expressed in a common coordinate system. Hence, a transformation from satellite's position expressed in CIRS to CTRS is performed before making range measurements. Yet, satellite navigation messages, which contain the key parameters required from receivers to compute their position, are already set to the CTRS system to avoid receiver from performing an extra rotation operation. Nonetheless, once the receiver obtains the Cartesian coordinates corresponding to its position, another conversion must be performed to obtain measures which are intuitive for a user, that is, a user would understand much better a coordinate expressed in terms of latitude, longitude and altitude than Cartesian coordinates (X, Y, Z), which might all vary at the same time if only the user moved its altitude.
Both GPS and Galileo use the same reference models but with their own variations, which among other things include a set of corrections. In the case of GPS it is used the World Geodetic System from 1984 (WGS 84) [20], which is a realisation from the CTRS. On the other side, Galileo does the same and uses the Galileo Terrestrial Reference Frame (GTRF) [11]. In figure 2.5 obtained from [21], the two terrestrial and inertial reference systems from Galileo's GTRF are compared so as to give a graphic idea of their design. More information about GNSS reference systems can be found in [22].

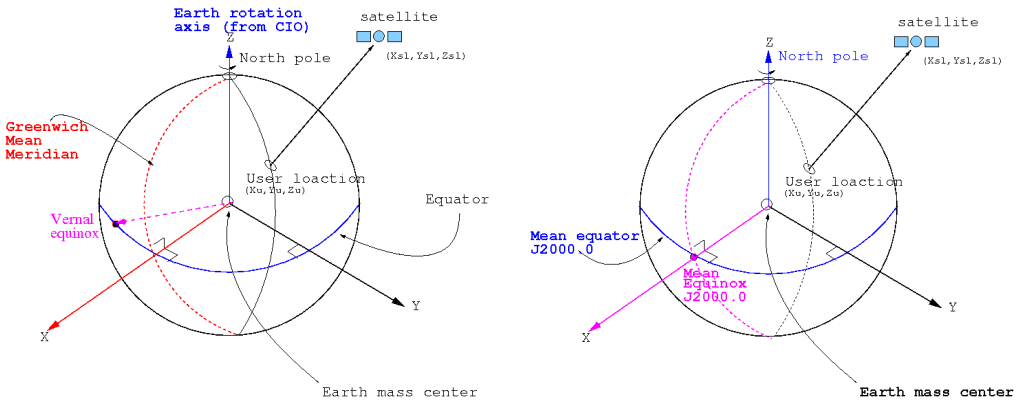

Figure 2.5: TRS and CRS coordinate frames.

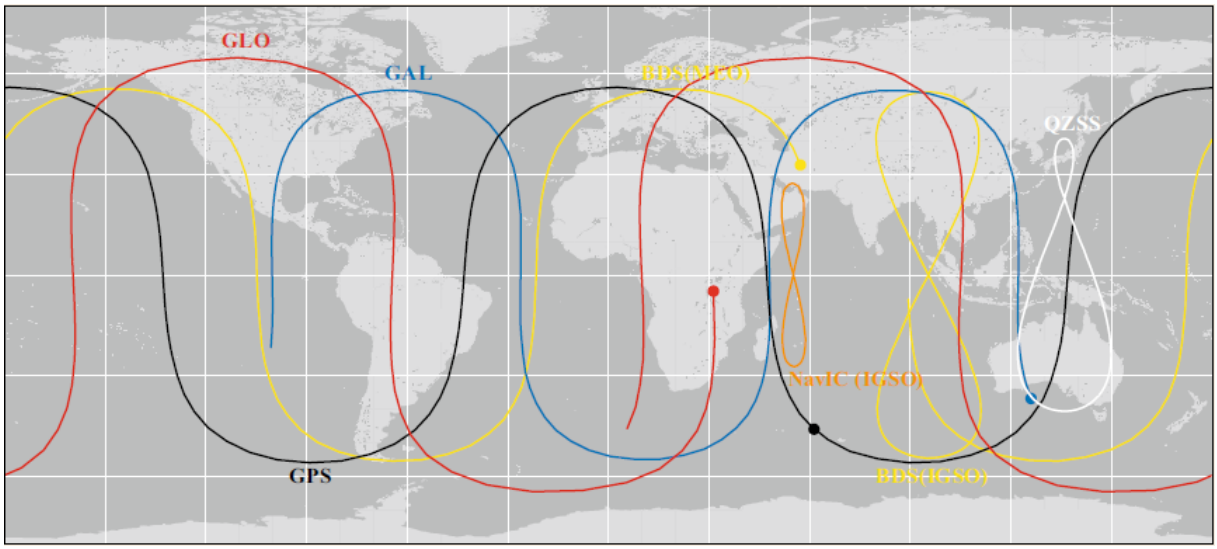

Figure 2.6: Examples of satellite orbit traces from different GNSSs.

Satellites were placed in space to follow specific and well known orbits, so that it is much easier to know their position at any time. Thanks to this, base stations from the control segment are able to keep track of satellites and to upload them periodically new sets of ephemeris, which will be later re-transmitted via satellite navigation messages during a certain time period. With ephemeris' parameters regarding orbits and a time reference, receivers are able to reconstruct satellite positions to later perform range measurements. A set of orbits from different GNSS are displayed in figure 2.6, from [23] (ch.3.3.1), in order to give an idea of the trace satellites leave whilst rotating the earth.

In the above paragraphs, it has been explained that GNSSs use reference systems to represent and compute positions, and that the parameters which describe satellite orbits are obtained from the navigation message. These two concepts have in common that they depend on a time reference, which is a very important parameter in GNSSs. All satellites and receivers are as synchronised as possible to a time reference, which is usually controlled by very precise atomic clocks in satellites and control stations. Errors in this reference could incur in hundreds of meters in measurements. For example, if a receiver measured time time of arrival of a satellite signal with a timing error of +1 second, the consequent measured range would be $(v * 1s) = 299\ 792\ 458$ meters longer than the actual one (considering that v is the speed of light in m/s.), which would not represent the real user position and thus would introduce severe errors in the final solution.

	GPS			Galileo		
	L1 C/A	L2C	L5	L1C	E1 OS/E5b	E5a
Message ID	*NAV*	*CNAV*	*CNAV*	*CNAV-2*	*I/NAV*	*F/NAV*
Block terminology	Subframe	Message	Message	Frame	Word	Page
Block length [bits]	300	300	300	883	260	256
Preamble [bits]	8	8	8	0	20	12
Parity/CRC/Tail [bits]	60	24	24	48	36	30
Block duration [s]	6	12	6	18	2	10
Bit rate [bps]	50.0	25.0	50.0	49.1	130.0	25.6
Effective bit rate [bps]	**38.7**	**22.3**	**44.7**	**46.4**	**102.0**	**21.4**
Efficiency factor [%]	77%	89%	89%	95%	78%	84%

Figure 2.7: GPS and Galileo Navigation messages compared.

Both receivers and satellites have clock errors, however, satellite clock errors are precisely know and are provided in the ephemeris from the navigation message so as the receiver takes them into account when computing its position. Receiver's clock need to be estimated in the positioning algorithm as it will be demonstrated in section 2.4. Both the GPS and the Galileo are defined as a week number plus the number of seconds of the week. The week starts at midnight between Saturday and Sunday whilst week seconds go from 0 to 604,800s (seconds in a week). A curious fact from GPS time reference is that, as its week number uses a 10 bit word in the navigation message, every 1023 these bits need to be restarted to 0 to keep the week count. This fact is called week rollover, and the last time it happened was last April 6^{th} of 2019.

As it has been repeatedly mentioned, the key parameters which allow receivers to

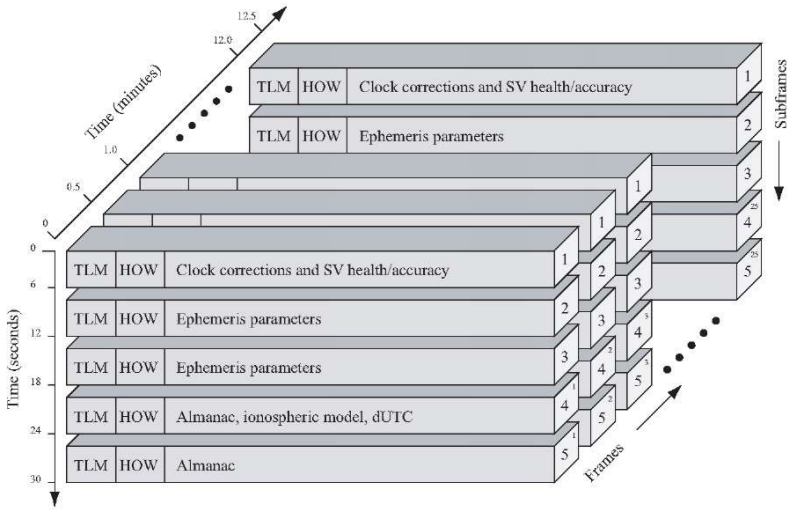

Figure 2.8: GPS navigation message organization.

compute their positions are contained in the ephemeris that satellites transmit via the navigation message. The latter, is divided in categories and each category contains different types of parameters.

- **Ephemeris:**
  Indicate the position of the satellite with a set of orbital parameters.

- **Time and Clock correction:**
  These parameters allow receivers to calculate LoS measurements.

- **Service Parameters:**
  These are needed to identify the set of navigation data, satellites, and indicators of the signal health

- **Almanac:**
  Indicate the position of satellites with a reduced accuracy.

GPS and Galileo navigation messages characteristics are different and count with different configurations depending on the bands in which they are transmitted. Its main characteristics are gathered in picture 2.8 extracted from [24].

With respect to the navigation message organisation, a GPS navigation frame is taken as an example to show its basic structure (see figure 2.8). A frame requires 30 seconds to be transmitted and it is divided into 5 sub-frames. Thus, each sub-frame lasts 6 seconds and contains 10 words in it. Sub-frames 1-3 contain satellite clock corrections, health indicators, age of data and satellite ephemeris. As they are the most relevant data from the navigation message, they are repeated from frame to frame. Sub-frames from 4-5 contain additional information about the ionosphere and almanacs. Inside each sub-frame (from 1 to 5), there are two special words; Telemetry word and Hand-over word, TLM and HOW respectively. TLM contains a synchronisation pattern, which is used by receivers to keep synchronised while decoding navigation messages. On the other hand, the HOW contains the Time of Week (TOW) or the number of 6-second sub-frames since the beginning of the week and start of transmission of the next sub-frame.
For more detailed information about GNSS coordinates, time and orbits, see [25], [26] and [27]

2.4 Estimation of position

The main goal of this section is to explain how does the receiver use the information provided by satellite signals and to describe the positioning algorithm in detail.
The principle of GNSS positioning is based on the 3D trilateration technique. In the latter, receivers basically calculate different signal times of a arrival to relate them to distance measurements. The latter are input parameters to the equations system which describes the user position. Its output are the Cartesian coordinates which fit best the proposed equations system.

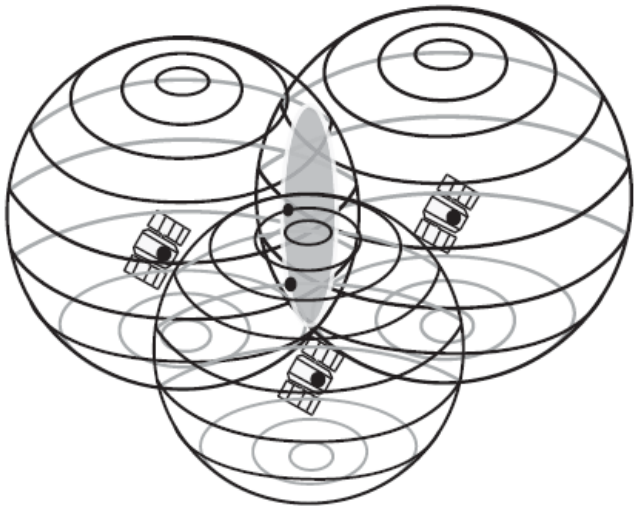

Figure 2.9: Satellites performing the trilateration technique.

Imagine the receiver only calculates one distance measurement. In this situation, the only information it obtains is that it is located somewhere along a sphere radius, which is has its centre in the corresponding satellite. However, if it calculates more than one distance measurements, the corresponding spheres would cut each other, as it is shown in figure 2.9 from [28]. The common point in which all spheres cut coincides with the user location. The process to formulate each range equation is graphically described in figure 2.10 for a 2D space, where y' and x' are the corresponding X and Y components of the LoS. The range itself can be expressed as the hypotenuse using basic trigonometric rules, that is:

$$h = \rho = \sqrt{x'^2 + y'^2}$$

being ρ the corresponding range. Considering x' and y' are a measure of distance between the receiver's and the satellite position, it can be expressed in the following way:

$$\rho = \sqrt{(x_s - x_r)^2 + (y_s - y_r)^2}$$

Where the subscripts s and r refer to satellite and receiver coordinates respectively.
This process would fit a 2D model, in which the range describes a circumference around the satellite. The equivalent equation using a sphere instead of a circle, and thus including an additional coordinate to fit the 3D model would be the following:

$$\rho = \sqrt{(x_s - x_r)^2 + (y_s - y_r)^2 + (z_s - z_r)^2} \tag{2.1}$$

This equation corresponds to the basic navigation equation. Which, for simplicity, is usually expressed as:

$$\rho = ||X_s - X_r||$$

Being X_s and X_r satellite and receiver Cartesian coordinates.
As mentioned above, more equations describing the range from receiver to the satellite within the corresponding sphere are needed so that they provide the receiver's position with their intersections. A priori, as ρ and X_s are known, it could seem that only three equations are needed to solve for the user position X_r. However, Satellite and receiver clocks are not perfectly synchronised. Typically, receiver clocks count with cheap and inaccurate clocks, which means they will be biased from the reference GNSS time. This biases impede the accurate determination of ranges causing error in position estimates.

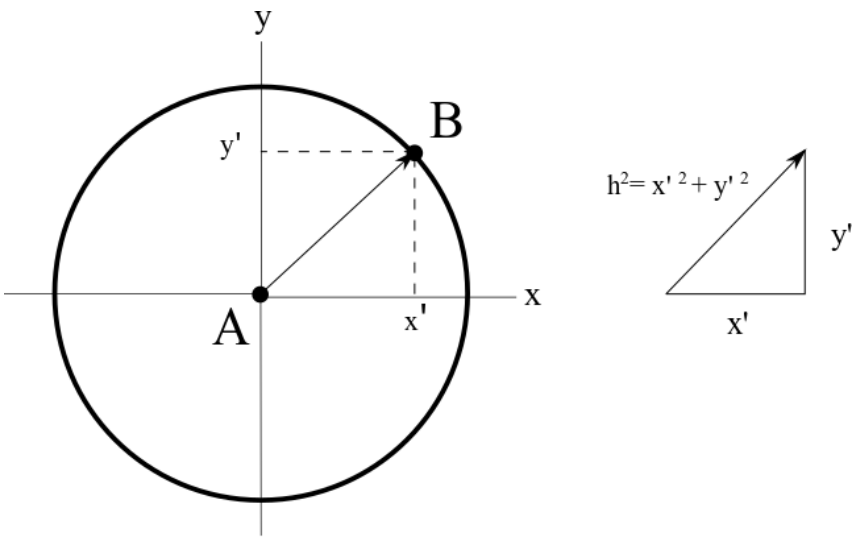

Figure 2.10: Forming 2D range measurements using basic trigonometric rules.

For this reason, it needs to be compensated. To do so, an additional unknown will be introduced to the equations system, as the receiver does not know a priori its time difference with respect to GNSS time.
Finally, the system is described by a set of, at least, four equations with for unknowns each other, as:

$$\rho^{(k)} = ||X_s^{(k)} - X_r|| + c \cdot t_b + \epsilon^{(k)} \tag{2.2}$$

Where $\epsilon^{(k)}$ gathers all measurement errors and t_b accounts for the receiver clock offset (with respect to the satellite clock) in seconds. The subscript k is used to distinguish between different satellite measurements.
A simple approach to solve these non-linear K equations is by using the so-called Least-Squares (LS) algorithm [29]:

$$\rho^{(k)} - \hat{r}^{(k)} = -\frac{(x^{(k)} - \hat{x}_r)}{\hat{r}^{(k)}} \cdot \Delta x_r - \frac{(y^{(k)} - \hat{y}_r)}{\hat{r}^{(k)}} \cdot \Delta y_r - \frac{(z^{(k)} - \hat{z}_r)}{\hat{r}^{(k)}} \cdot \Delta z_r - c \cdot t_b \tag{2.3}$$

Where $\hat{r}^{(k)}$ stands for:

$$\hat{r}^{(k)} = \sqrt{(x_s - \hat{x_r})^2 + (y_s - \hat{y_r})^2 + (z_s - \hat{z_r})^2}$$

And $\hat{x}_r$, $\hat{y}_r$ and $\hat{z}_r$ will be the a initial position in the fist iteration, typically denoted as (x_0, y_0, z_0).
Expression 2.3 can be expressed in matrix form by taking into account the following considerations:

$$e_x^{(k)} = -\frac{(x^{(k)} - \hat{x}_r)}{\hat{r}^{(k)}}, \quad e_y^{(k)} = -\frac{(y^{(k)} - \hat{y}_r)}{\hat{r}^{(k)}}, \quad e_z^{(k)} = -\frac{(z^{(k)} - \hat{z}_r)}{\hat{r}^{(k)}} \tag{2.4}$$

$$H = \begin{bmatrix} e_x^{(1)} & e_y^{(1)} & e_z^{(1)} & 1 \\ \vdots & \vdots & \vdots & \vdots \end{bmatrix},$$
$$\Delta_x = \begin{bmatrix} \Delta x_u & \Delta y_u & \Delta x_z \end{bmatrix}^\intercal \tag{2.5}$$

Thus, the resulting system of equations is:

$$\Delta\rho = H\Delta x$$

In the case four measures were obtained, H, which is usually called the Geometry Matrix, would be a square matrix and thus invertible. However, it is of great interest to add more satellite measurements to the equation in order to obtain more accurate estimates. For this, the procedure to solve the equation is by using the Least Squares (LS) method, which is detailed in [29] and [28] (ch.7.3). The LS algorithm is an iterative method, which aims to reduce the mean-squared-error, results in:

$$\Delta x = (H^T H)^{-1} H^T \Delta\rho \tag{2.6}$$

This equation will be solved iteratively. At each iteration, the defined initial state, which is composed by the user a priori position and the receiver's clock bias, will be updated. After each initial position update, the equations will be again linearised over this new point to obtain a new LS solution, until a convergence point is reached. The convergence is said to be obtained when differences between measured and computed pseudoranges (often called residuals) do not decrease between different consecutive iterations, or equivalently, when the obtained update to the initial position does not change. If this happens and if all goes well, the a priori position has been updated correctly to the actual position.

2.5 Measurement errors and error sources

This section is aimed to do a brief review of the existing error sources which affect GNSS positioning, so shed light to GNSSs imperfections. This information was mainly extracted from [28](ch.7) and [8](ch.5). Some of these error sources, specially Ionosphere effects will be explained in more detail in chapter 3. To summarize, measurement errors can be divided in the following sections:

- **Receiver noise:**
  The receiver noise makes reference to errors induced by the receiver tracking loops and have impact mainly in measured pseudoranges. The dominant sources of error are basically thermal noise jitter and interference effects. These effects however do not affect equally code and phase measurements. As it will be demonstrated in further sections, carrier phase measurements are less noisy and thus constitute of a more precise measure. Yet, these measurements are ambiguous and should be treated in a special way.

- **Multipath:**
  Multipath is one of the most remarkable errors from the receiver perspective. These errors are due to multiple replicas of the same signal arriving at the receiver in different time stamps, producing interference and misleading the receiver. Multipath is more difficult to mitigate than other error sources and its error magnitude depends on the scenario. The more obstacles the scenario has, the more reflections will the signal suffer, increasing the number of paths for the same signal.
  It is worth mentioning that multipath do not affect equally to all GNSS signals, in fact, it is expected that the higher the chipping rates, the higher the signal's robustness against it.

- **Hardware biases:**
  Hardware biases result from either satellite and user equipment biases. On the one side, the different satellite signals are not perfectly synchronised among each other. Different modulations and/or frequency bands count with slightly different delays across hardware components, which traduce in measurement errors. On the other side, user equipment delay signals and are also frequency dependent.

Another error source of considerable magnitude is the Earth's Atmosphere. The Atmosphere is divided into layers which affect and degrade differently satellite radio-signals. Its most relevant layers in terms of error sources are Troposphere and Ionosphere. The latter, constitutes one of the greatest error sources in positioning for common receivers.

- **Troposphere effects:**
  The Troposphere is the earth's lowest layer and contains most of the atmosphere's mass. It extends from about 10km to 40km from the earth's surface. It is a refractive medium, thus, the phase and group velocities associated to GNSS carrier signals will be delayed. This delay is a function of the troposphere refractive index, which depends on the local temperature, pressure and relative humidity, but it is not frequency dependent like the Ionosphere. Troposphere effects can be divided into two subsections, the wet and dry components. Both components are usually compensated effectively using models, however, the wet component, which arises from the water vapour is more difficult to predict and therefore may introduce more error. If Troposphere effects were left uncompensated, they may introduce an error in between 2.4 and 25 meters according to [8]. More detailed information can be found in [8] (ch. 5.3.3).

- **Ionosphere effects:** The Ionosphere is a dispersive medium located in between 70km and 1000km from earth's surface. The delay introduced in signals during their path through ionosphere is generally greater in magnitude than troposphere delays, and additionally, it will depend on the signal's carrier frequency. In contrast to Troposphere, Ionosphere delays are more difficult to predict using models, so it becomes a greater threat for position accuracy.
  Each satellite constellation counts with its own models for compensating Ionosphere effects. In the case of GPS, navigation messages include data which serve as parameters for its Klobuchar Ionosphere model. This model compensates about the 50% of Ionosphere error in measurements, according to [25]. Galileo on its side, uses an adaptation of the Nequick Ionosphere model, named Nequick-G. According [30], this model is expected to correct around 70% of Ionosphere effects , which means it outperforms the Klobuchar model. However, this comes at a price, as this model is in general more resource-demanding. As mentioned earlier, aspects concerning the Ionosphere layer effects will be explained in more detail in chapter 3.

Chapter 3

Dual-Frequency measurements for positioning

The content of this chapter is divided in two sections. The first one describes briefly GPS and Galileo signals available for positioning and points out the benefits obtained from them for navigation purposes. Its main goal is to analyse different signal properties from a theoretical perspective and compare them in terms of expected accuracy and robustness to error sources.

Signal redundancy allows receivers to combine its measurements to compute estimates of one of the most considerable error sources in satellite positioning, which is the ionosphere error. The latter is the topic of the second section of this chapter. Here, elements which characterise them are analysed also from a theoretical approach, with the aim of clarifying their provenience and the parameters from which they depend.

Later in chapter 4, signals here mentioned will be tested and compared. Also, various ionosphere error mitigation techniques based in the theory explained in the second section of this chapter will be tested, to evaluate dual frequency measurements impact in positioning and see the best options to combine them so as to improve positioning accuracy.

3.1 GPS and Galileo signals

As mentioned earlier, this section is aimed to do overview of GPS and Galileo signals in terms of PVT accuracy. With this, we will be able to later extract conclusions from the tests performed in chapter 4.

3.1.1 GPS L1 & L5

The first GPS satellite signals (legacy signals) where located in L1 (1575.42 MHz) and L2 (1227.60 MHz) bands for civilian and military applications, respectively. Satellite signals located at the L1 band use *coarse/acquisition* (C/A) PRN codes, which are Gold codes with a period of 1023 chips transmitted at 1.023 Mchip/s, causing the code to repeat every 1 millisecond. According to [31], these signals are expected to provide accuracies from 5 to 10 meters for stand-alone receivers which only use satellite signals, i.e without assested or augmented systems), down to 0.7 to 0.3 meters for those using differential data.

On the other side, the new GPS L5 signals located in the L5 band (1176.45 MHz), count with different PRN codes of 1 millisecond in length at a chipping rate of 10.23 Mbps. As it is pointed out in bold letters in table 3.1, these signals are received at a higher power than L1 and also count longer spreading codes. Besides, they count with improved modulation techniques considered better in terms of error probability in equal conditions. For this, they are expected to improve L1 performance when used for positioning. That being said, the inclusion of these new signals are still under development, and form part of the GPS's modernisation plan started in 2010 [3]. Later on, it will be seen that the lack

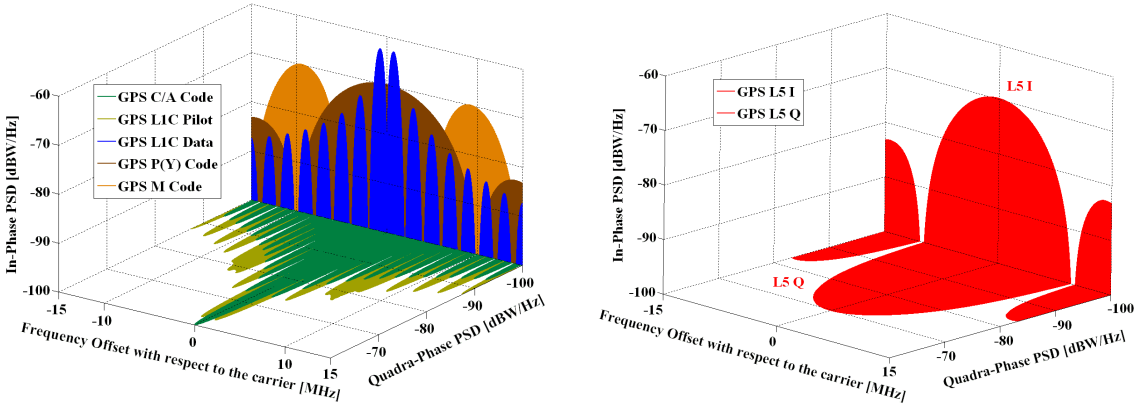

Figure 3.1: GPS L1 and GPS L5 signals spectra.

Frequency Band	L1	L5
Centre Frequency(MHz)	1575.42	1176.45
Access technique	CDMA	CDMA
Spreading modulation	**BPSK(1)**	**BPSK(10)**
Code Frequency(MHz)	**1.023**	**10.23**
Primary Code length	**1023**	**10230**
Minimum received power [dBW]	**-158.5**	**-157.9**
Bandwidth [MHz]	**15.345**	**12.5**

Table 3.1: GPS Signal plan

of satellites counting with these measurements will constrain the system performance. See [32] for more information about GPS's L5 signals.
Images 3.1 were obtained from [33] and reflect GPS L1 and L5 signals spectrum.

3.1.2 Galileo E1 & E5

According to [26], Galileo satellites transmit permanently three independent CDMA and Right-Hand Circularly Polarised (RHCP) signals, named E1, E5 and E6. However, E6 signal has not been available for civilians until recently, so it will not be considered in this research. The E5 signal is further divided in two signals denoted E5a and E5b. Each signal is allocated differently within the spectrum as it can be seen in figure 3.2 from [26] (ch.2.1.1). Galileo's signals transmitting in E5 and E6 bands are not a system novelty.

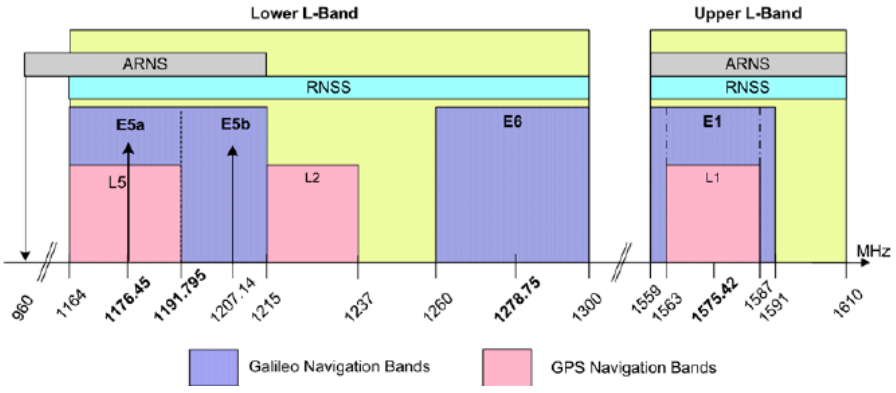

Figure 3.2: Galileo frequency plan

Frequency Band	E1	E5(a,b)
Centre Frequency(MHz)	1575.42	1191.795
Access technique	CDMA	CDMA
Spreading modulation	**CBOC(6,1,1/11)**	**ALTBOC(15,10)**
Code Frequency(MHz)	**1.023**	**10.23**
Primary Code length	**4092**	**10230**
Minimum received power [dBW]	**-157**	**-155**
Bandwidth [MHz]	**32**	**23.205/27.795/ 40**

Table 3.2: Galileo Signal plan

They have been included in satellites since the fist launchment took place in October 2011, in contrast to GPS's L5 band. That being said, as Galileo's satellite constellation has been for years under development, their availability has been increasing progressively. At the reporting date, Galileo's constellation is about to be considered fully operational somewhere between 2019 and 2020. For more detailed information, see [4].

In the first place, the E1 signal for civilians has a 4092 code length with a 1.023 MHz chipping rate giving it a repetition rate of 4 ms. In the second place, E5 counts with 10230 PRN code length with 10.23 MHz chipping rate. As in the case of GPS, E5 signals are receiver at a higher power than E1 signals, and also count with longer spreading codes and improved modulations which are expected to reduce error probability in equal conditions.

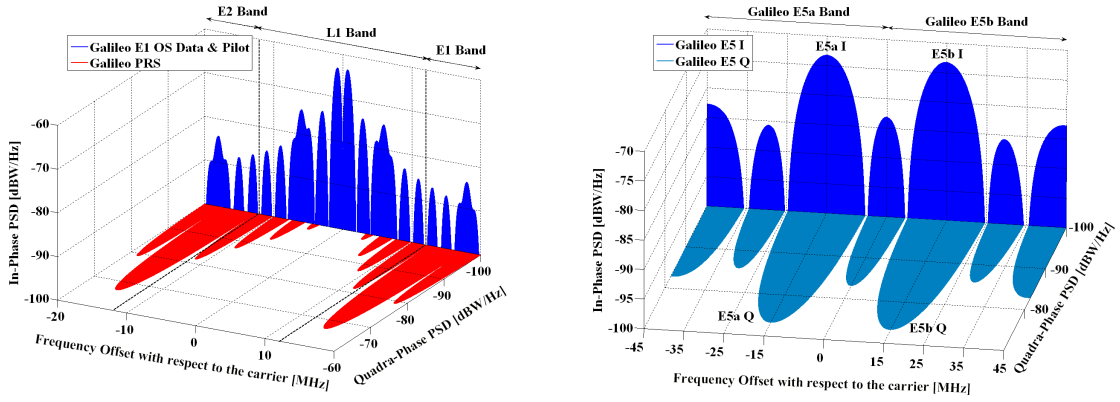

Figure 3.3: GAL E1 and GAL E5 signals spectra.

Another important consideration for both GPS and Galileo signals is that, according to [23], higher chipping rates is associate to better resolution and less multipath error in measurements, which constitute another advantage from L5/E5 with respect to L1/E1.
In figure 3.2 it is noticeable that E5a and E5b do not count with wider BWs than E1 signals. However, they can be treated as a single signal (E5ab) to take advantage of their total combined BWs. Wider BWs are related to higher processing gains, which allow receivers to make more accurate estimates in the acquisition and tracking stages (see [34]). Figures from 3.3 were extracted from [35] and reflect both Galileo E1 and E5 signals spectra.
It is proved in [36], that positioning results obtained using E5 signals can outperform those from E1, specially when using the full E5 signal.

3.2 Dual Frequency PVT

In the previous section, it has been mentioned that signals in L5 and E5 bands count with better characteristics for navigation. However, there are various reasons which justify that nowadays the main measurements sources are L1 and E1 bands from GPS and Galileo, respectively. On the one hand, receivers have been historically limited to navigate using the GPS civilian L1 band. With the arrival of Galileo in 2003 together with the approval of the GPS modernisation plan in 2010, the number of available signals was progressively increased, which started to justify the deployment of receivers compatible with L5 and E5 bands to benefit from their characteristics to improve navigation accuracy. On the other side, either L1 and E1 signal characteristics, e.g. chipping rates, relax receiver's hardware requirements, which make them ideal for common receivers which accept standard position accuracies. Besides, the same hardware user for processing GPS L1 signals can be used for Galileo E1 signals.

Receivers willing to benefit from L5 and E5 signal characteristics should first take into account various considerations. In the first place, they should evaluate if their signal processing and hardware capabilities are enough to cope with these signals. In the second place, receivers should count with the means to mitigate ionosphere effects as they affect in greater measure in L5/E5 bands (see section 3.3.3). If these considerations are validated, navigation using L5/E5 signals should be prioritised over L1/E1. An aspect worth mentioning in this context is that GPS L5 signals are insufficient to provide receivers with an adequate set of measurements to perform navigation. Nearly all L5

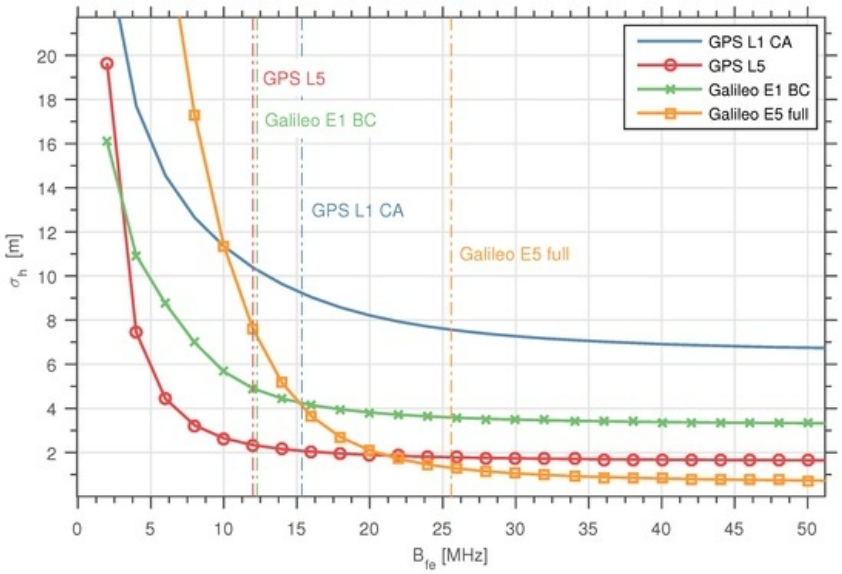

Figure 3.4: CRB - GPS L1/L5 and GAL E1/E5

visible satellites per epoch should be used in order to be able to solve the positioning algorithm, this implies little signal redundancy, and prevents GPS receivers from rejecting those satellites located in low elevations or which measurements bias positioning results due to its bad measurements.

Finally, counting with DF measurements, arises the possibility to combine them so as to subtract ionosphere delay from the signal in the selected reference frequency. However, as it will be seen in the next section, this procedure introduces noise in the resulting measurements. For this, its application should depend in the particular characteristics of each scenario. DF measurements will be useful in scenarios where ionosphere errors are predominant and the maximum level allowed of measurements noise is not very restrictive, because the amount of correction applied to measurements is greater than the noise contribution. On the contrary, in the opposite scenario, it would be a better option to discard DF measurements and simply make use of broadcast models which are not as effective correcting ionosphere errors but introduce less amount of noise.

Figure 3.4 was obtained from [37] and shows by means of the so called Cramér-Rao lower Bound [38], the minimum amount of error expected in each of the above mentioned signals from GPS and Galileo. It is proved that higher positioning accuracy are expected using L5 and E5 bands, specially in the combination of E5a and E5b. As it will be seen in the next chapter, in order to see these improvements all positioning errors of greater magnitude should be compensated, which is not an easy thing to do.

3.3 Ionosphere Delay estimation

As in stated in section 2.5, this part has taken [8] and [28] as a reference to consult and verify the procedures below followed.
The Ionosphere is a dispersive medium, which is located from 70km to 1000km above Earth's surface. It is basically composed by light gases, whose atom's electrons have been stripped of an indeterminate number of electrons due to solar and cosmic radiation. The ionised electrons behave as free particles, which influence electromagnetic wave propagation, and therefore GNSS radio-signals, modifying the medium's refraction index and delaying them.

3.3.1 Ionosphere effects

The amount of signal delay in terms of group and phase velocity caused by free electrons in the Ionosphere, can be obtained by relating the medium's index of refraction and the signal frequency as:

$$v_p = \frac{c}{1 - \frac{40.3 n_e}{f^2}}, \quad v_g = \frac{c}{1 + \frac{40.3 n_e}{f^2}} \tag{3.1}$$

Being c the speed of light and n_e the medium's refraction index. Subscripts p and g refer to phase and group respectively.

In the above equation, it is possible to see that, whereas the signal's group velocity is delayed, the phase velocity is advanced due to free particles. This is basically the so-called ionosphere effect. As the index of refraction varies along the ionosphere, the signal's group and phase velocity will do the same along the signal path through ionosphere. Finally these velocity variations along the signal path delay its travel time. With this in mind, the total delay can be expressed in meters in the following way:

$$\Delta I_p = -\frac{40.3}{f^2} \int_{sv}^{rcv} n_e dl, \quad \Delta I_g = -\frac{40.3}{f^2} \int_{sv}^{rcv} n_e dl$$

Where subscripts rcv and sv stand for the correspondent satellite and receiver positions, to measure the signal path from the satellite to the receiver.
As the electron density along the path is called total electron content (TEC), the above equation can be redefined as:

$$I_p = -\frac{40.3}{f^2}TEC, \quad I_g = +\frac{40.3}{f^2}TEC \tag{3.2}$$

Where TEC is expressed in units of units of $electrons/m^2$.
Equation 3.2 contains the basic equations that characterise the resulting phase and group signal delay due to the ionosphere's layer freed-up electrons. It seems clear that the longer the signal path through the ionosphere layer, the greater will the TEC value expected be. In other words, the signal path within the ionosphere layer will depend on its angle angle incidence, as it is represented in figure 3.5, from [28] (ch. 7.2.4.1), and is accounted for by the so called *Obliquity Factor*.

This fact is proved in figure 3.6, where the same RINEX file from section 4.1 has been used to display GPS PRN 1 Satellite's elevation for a time period of approximately 4 hours, together with its TEC estimates, which were obtained from combining Dual-Frequency (DF) measurements, for the same time period. In this figure it is noticeable that, when PRN 1 counts is located in low elevations with respect the reference station (RS) local horizon, its TEC estimate is greater. On the contrary, as the satellite approaches to the RS's zenith its TEC estimates decrease in magnitude, and again

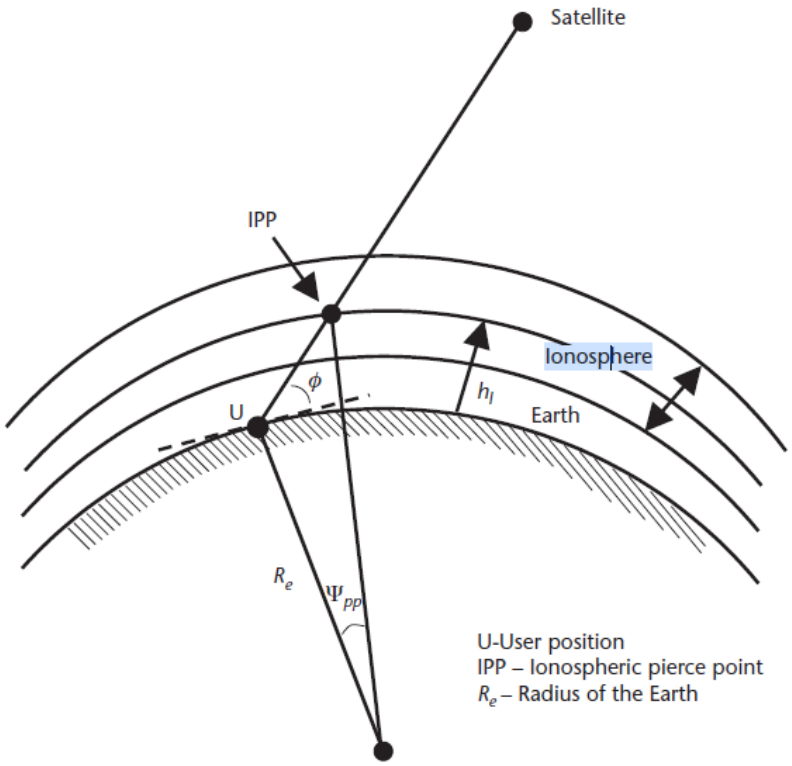

Figure 3.5: Radio-Signal's Obliquity factor

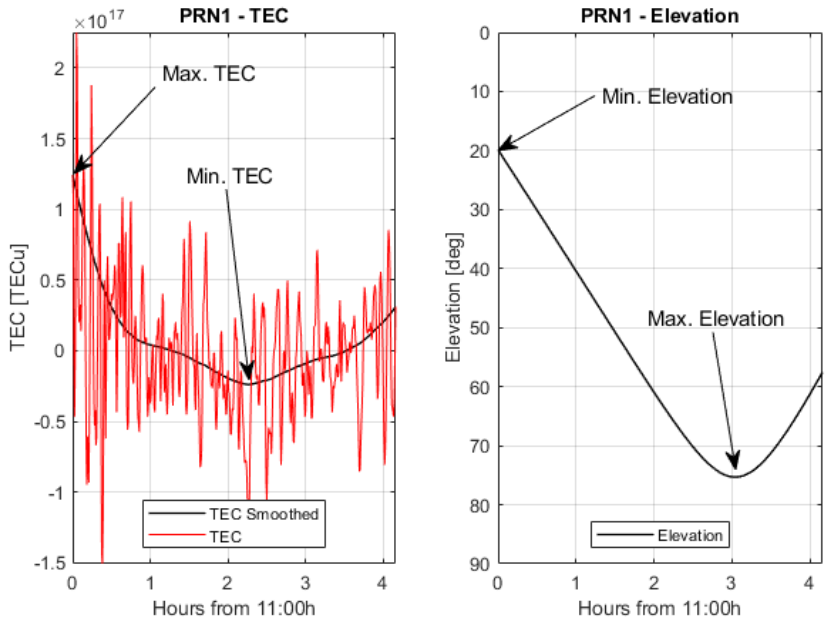

Figure 3.6: Relationship between estimated TEC and satellite elevation.

increases as it surpasses it and moves away.

At this point, one could deduce that ionosphere effects depend on the receiver's position and time of the day. This is because on the one side, as aforementioned, solar radiation affects in greater measure in zones close to the Earth's equator. On the other side, its effects upon regions vary along the day, that is, at night, as less solar radiation is present in the ionosphere, less density of freed-up electrons will it contain, reducing the expected ionosphere delay in satellite radio-signals. Besides, solar cycles are another

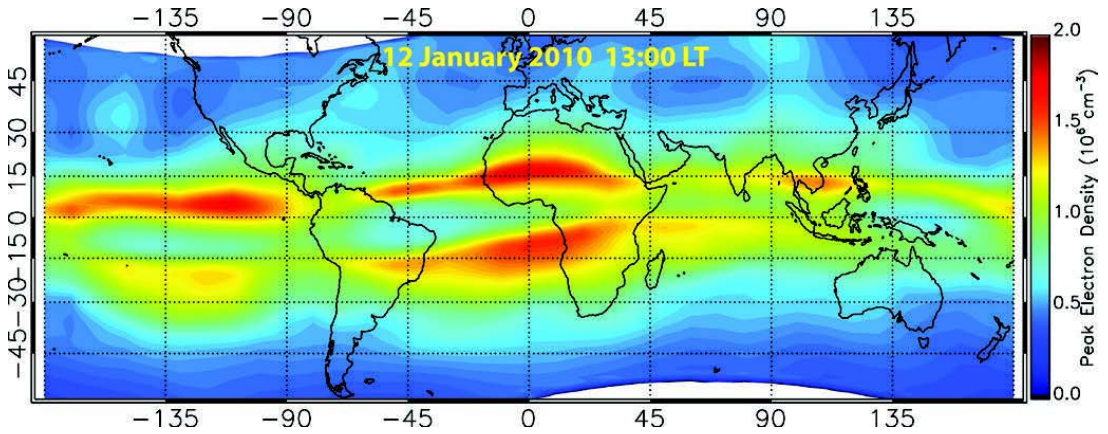

Figure 3.7: Ionosphere's electron densities due to solar radiation.

aspect to take into account as they also increase or decrease the overall ionosphere effects for its duration period.
In terms of Ionosphere spatial variation, several institutions such as the US Naval Research Laboratory, measured solar radiation upon earth (see figure 3.7), where it is possible to see that for regions located in the equator, the intensity of the solar radiation in much stronger than in zones nearer to the poles.

3.3.2 Delay estimation for SF receivers

As it has been mentioned previously, one approach to mitigate ionosphere errors from measurements without increasing the noise contribution is by obtaining error estimates from broadcast models. As explained in section 2.5 either GPS and Galileo count with its own model approaches. Galileo on its side implements the Nequick-G model [30], which is accurate, but also more complex and resource demanding than GPS's Klobuchar [39]. The latter is much more simple model, but the amount of error it subtracts from measurements is less in comparison to Nequick-G. This research will focus on the Klobuchar model, which will later be applied either separately and in combination with DF corrections in order to increase the amount of correction in the GPS case, which had the limitations of counting with a reduced fleet of satellites with DF measurements.

The Klobuchar model is the GPS's Ionosphere broadcast model which takes as inputs key parameters contained in the ephemeris and provides receivers with ionosphere error estimates. Although this model is mainly aimed to SF receivers, it can also be used for DF receivers to remove Ionosphere error more effectively, as it will be seen in chapter 4.
As it is stated in [25] and [8], the Klobuchar model represents the zenith delay as a constant value at nigh-time and a half-coisine funcition in day-time. Its estimate is provided by the following function:

$$\frac{\hat{I}}{c} = \begin{cases} A_1 + A_2 \cdot cos(\frac{2\pi(t-A_3)}{A_4}), & if\ |t-A_3| < A_4/4 \\ A_1 \quad otherwise \end{cases}$$

where:
A_1 is the night-time value of the zenith delay, which is fixed at $5x10^{-9}$, A_2 is the amplitude of the cosine function for day-time values, A_3 is the phase, corresponding to the peak of the cosine function, which is fixed at 14:00h at local time, and A_4 is the period of the

cosine function.
As aforementioned, the values which are not already fixed and required to obtain an estimate from this model are specified in the navigation message broadcasted by each satellite, in terms of four coefficients. The resulting ionosphere error estimates from the RINEX mentioned in section 4.2 to compute the positioning are displayed in figure 4.11. It can be seen that Ionosphere error estimates reach their maximum at approximately 14:00h, considering that the figure comprises a time period between 00:00h and 23:59h and the middle corresponds to 12:00h.
For more information about the GPS's Klobuchar model, the reader is again referred to [25] and [39].

3.3.3 Delay estimation for DF receivers

In equation 3.2 the expression regarding the ionosphere delay was obtained; only one expression for two unknowns, which are the TEC and the ionosphere delay itself noted as I. In order be able to solve for I, two different frequency measurements from the same satellite should be taken and combined appropriately. With this combination, it is possible to obtain a very accurate estimate (99.9% according to [8] and [40]) and later remove it from range measurements.
This procedure is done as follows:

$$\rho_{(f)} = \rho^{IF} + I_{(f)} + t_b + \epsilon \tag{3.3}$$

Where:
$\rho_{(f)}$ is the actual measured pseudorange, ρ^{IF} is the ionosphere-free pseudorange, $I_{(f)}$ is the ionosphere error in the selected frequrency (f), t_b is the clock bias in meters and ϵ_f gathers measurement errors of the selected frequency.
For simplicity, it will be assumed that the receiver clock bias is well estimated and removed in the receiver. Relating the above equation with 3.2 it is obtained:

$$\rho_{(f)} = \rho^{IF} + \frac{A}{f^2_{(f)}} + t_b + \epsilon \tag{3.4}$$

Where $A = 40.3 \cdot TEC$, and the rest of the parameters are defined above in 3.3.
For simplicity, let's assume that the pair of frequencies we are working with are the L1/E1 - L5/E5 bands which will be denoted as 1 and 2.
In 3.4, we count with one equation and two unknowns: ρ^{IF} and A. However, by using

the equation for each frequency band, it is possible to remove common measurements and obtain an estimate for A by taking one frequency as a reference, that is:

$$\begin{aligned} \rho_{(i)} &= \rho^{IF} + \frac{A}{f_i^2} + \epsilon \\ \rho_{(j)} &= \rho^{IF} + \frac{A}{f_j^2} + \epsilon \end{aligned} \tag{3.5}$$

leading to:

$$\rho_{(i)} - \rho_{(j)} = \frac{A}{f_i^j} - \frac{A}{f_j^j} \longrightarrow (\rho_{(j)} - \rho_{(i)}) \cdot \frac{f_i^2 \cdot f_j^2}{f_i^2 + f_j^2} = A$$

Notice, that measurement errors ϵ from both pseudoranges have been cancelled.
Now, depending on the frequency taken as the reference, the factor $\frac{f_i^2 \cdot f_j^2}{f_i^2 + f_j^2}$ will vary so as to provide the amount of error for the corresponding frequency.

$$\hat{I}(f_i) = \frac{A}{f_i} = (\rho_{(j)} - \rho_{(i)}) \cdot \frac{f_j^2}{f_i^2 + f_j^2} \tag{3.6}$$

With this equation, the ionosphere delay is estimated for the satellite signal at frequency f_i. However, there is another approach to directly obtain an iono-free estimate of the pseudorange at frequency $f(i)$, which is:

$$\rho_{(i)}^{IF} = \frac{f_i^2}{f_i^2 + f_j^2} \cdot \rho_{(i)} - \frac{f_j^2}{f_i^2 - f_j^2} \cdot \rho_{(j)} \tag{3.7}$$

These equations, allow receivers to substract ionosphere delay at a price, because when combining pseudorange measurements together, the resulting estimate becomes noisier. This fact becomes more notorious in the Ionosphere-free approach from 3.7, where according to [8] the noise contribution is increased by a factor of:

$$F = \sqrt{(\frac{f_i^2}{f_i^2 - f_j^2})^2 + (\frac{f_j^2}{f_i^2 - f_j^2})^2}$$

Where f_i and f_j are the pair of frequencies selected to perform the combination.
From the above equation we realise that the noise contribution will depend on the pair of frequencies selected, for example:

$$F_{L1L2} \approx 3$$

$$F_{L1L5} \approx 1.917$$

Being L1,L2 and L5 the different GPS frequency bands, which in case of L1 and L5 are equal to Galileo's E1 and E5.
As seen, F_{L1L5} will introduce less noise in the resulting measurements, and thus it seems the right choice for performing DF measurements.
From now on, L1 and L5 noting will refer to either L1/E1 and L5/E5 bands for simplicity.

Until this point, it has been explained how to compensate ionosphere effects by making use of DF measurements. However, there are several issues with this technique such as noisy corrections, poor DF satellites availability etc., which we aim to asses and test in the following chapter.

Chapter 4

Tests and results

The main objective of this chapter is to perform different positioning tests and compare the different obtained results, with the aim of pointing out the configurations and techniques that performs best in terms of position solution accuracy and ionosphere error mitigation, respectively.

The first part of this chapter will compare different signal configurations from either GPS and Galileo constellation. With this, it will be determined which is more adequate for obtaining accurate positioning results for each GNSS. At the same time, this comparison will allow to conclude which GNSS constellation performs best overall.

The second part will focus in mitigating ionosphere errors in measurements. For this, not only will techniques from chapter 3 be implemented separately, but also diverse manners to combine them will be tested with the aim of improving the final correction factor.

The data required for this tests will be obtained from RINEX files (see 4.1), and also from data logs obtained from a mobile phone with a DF compatible receiver integrated. The latter are composed by raw measurements, which imply that will be more noisy and difficult to treat.

4.1 Positioning using RINEX files

As in this research RINEX files have been profusely used to test different position configurations and scenarios, it is worthy to give them a quick glance in the current section.

The acronym RINEX stands for *Receiver Independent Exchange Format*. These files contain GNSS data collected by reference stations in a standardised format, so that users can use them to perform measurements and processing their data. The fact of providing GNSS data in a specific format, makes it easier for users to reuse their algorithms for different data sets, with different properties.
The parameters needed for receivers to compute their positions are contained in these RINEX files as it will be showed next.
On the one hand, all satellite ephemeris received for a specific time period are stored in the Navigation RINEX. These may include useful optional parameters, for example those aimed to fit GPS and Galileo broadcast models for compensating atmosphere effects. An example is displayed in figure 4.1 for satellite PRN 1. More information about how ephemeris are distributed in Navigaiton RINEXs is found in the RINEX's spread sheet [41].
On the other hand, measurements needed to compute a position are provided by Observation RINEXs and are often called *'Observables'*. Thanks to this, users do not have to calculate basic measurements from satellite signals' raw data. Instead, these are obtained directly from the *observables* provided by reference stations, which have already performed acquisition and tracking processes accurately. In figures 4.3 and 4.2 an example an Observable RINEX is displayed, where it is possible to see the structure in which the aforementioned parameters are organised. It is important to mention that

```
     3.02           N: GNSS NAV DATA    G: GPS              RINEX VERSION / TYPE
GR10 V3.11          Instituto Geografico20181013 235942 UTC PGM / RUN BY / DATE
GPSA   1.1176D-08  0.0000D+00 -5.9605D-08  0.0000D+00       IONOSPHERIC CORR
GPSB   9.0112D+04  0.0000D+00 -1.9661D+05  0.0000D+00       IONOSPHERIC CORR
GPUT  4.6566128731D-09 1.243449788D-14 233472 2023          TIME SYSTEM CORR
    18    18  1929     7                                    LEAP SECONDS
                                                            END OF HEADER
G01 2018 10 13 16 00 00-9.997701272368D-05-4.888534022029D-12 0.000000000000D+00
     6.100000000000D+01-1.656250000000D+01 4.173030966347D-09-2.722175588031D+00
    -1.046806573868D-06 8.118900936097D-03 1.048296689987D-05 5.153667583466D+03
     5.760000000000D+05 3.725290298462D-09 1.151578295630D+00-1.527369022369D-07
     9.726696685102D-01 1.829375000000D+02 6.989664338890D-01-7.704249484344D-09
     4.760912596834D-10 1.000000000000D+00 2.022000000000D+03 0.000000000000D+00
     2.000000000000D+00 0.000000000000D+00 5.587935447693D-09 6.100000000000D+01
     5.688000000000D+05
```

Figure 4.1: Navigation RINEX Example.

```
726336              LEIAR25.R4      NONE                    ANT # / TYPE
  4755888.2660    62302.1100  4236277.9720                  APPROX POSITION XYZ
        0.0770        0.0000        0.0000                  ANTENNA: DELTA H/E/N
G   16 C1C L1C D1C S1C C2S L2S D2S S2S C2W L2W D2W S2W C5Q  SYS / # / OBS TYPES
       L5Q D5Q S5Q                                         SYS / # / OBS TYPES
R   12 C1C L1C D1C S1C C2P L2P D2P S2P C2C L2C D2C S2C      SYS / # / OBS TYPES
E   16 C1C L1C D1C S1C C5Q L5Q D5Q S5Q C7Q L7Q D7Q S7Q C8Q  SYS / # / OBS TYPES
       L8Q D8Q S8Q                                         SYS / # / OBS TYPES
C    8 C1I L1I D1I S1I C7I L7I D7I S7I                     SYS / # / OBS TYPES
```

Figure 4.2: Observation's RINEX header key parameters.

the reference station approximate position is also included in the Observation RINEX's header; This parameter is of great relevance in order to compare the different positioning results with the actual one and test the accuracy of the positioning algorithm.
Users with the intention of using RINEX files for positioning need to build or download a RINEX reader so as to obtain its parameters. For this, as in this research more specific parameters than the basic ones for navigation where required to fit additional algorithms, i.e. Phase measurements, E5a/E5b and L5 measurements etc., a dedicated RINEX reader was designed to obtain and include them in the positioning algorithm.

RINEX files are of great convenience for users willing to perform tests using real GNSS data. However, these are not the only available data source. Another interesting way to obtain measurements and perform such tests is to work with mobile phone's data. In August 2016, with the new release of Google's Android 7.0, new APIs were introduced giving users access to GNSS raw measurements (see [5]). This fact allowed users to store data from their mobile phones so as to be able to process them using their own algorithms. That being said, mobile phone raw measurements must be treated more carefully than RINEX data, as its receivers are not as good as those from reference stations. In result, its measurements will be much noisier.

```
> 2019 02 14 00 00  0.0000000  0 38
G01  23541801.280   123712980.92506      2910.341          39.200
G07  25059950.700                       -1785.093          38.100
G08  20665285.760   108596818.20009      1232.668          55.050
G10  21281632.380   111835779.49308     -1307.946          52.700
G11  22965229.680   120683093.12007      2974.278          47.950
G14  25305242.160   132979952.60406      2737.367          41.350
G16  22808268.120   119858264.35808     -3433.182          49.650
G18  21237671.460   111604713.68908      2161.443          50.750
G20  22814543.080   119891281.85908     -2880.541          48.050
G21  26132369.060                       -2526.757          35.100
G22  24494796.200   128720987.40507      3623.686          47.100
```

Figure 4.3: GPS Observables in a RINEX file.

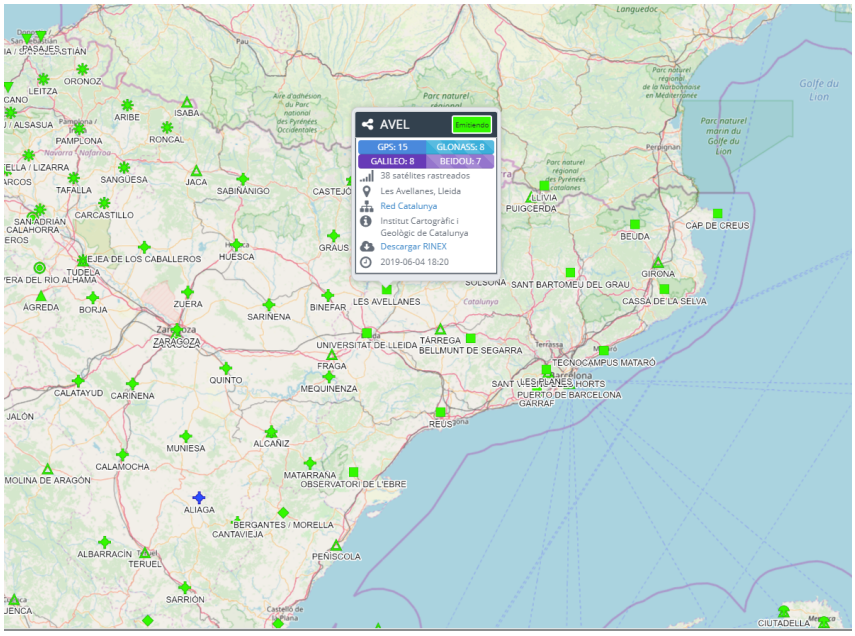

Figure 4.4: RINEX files reference station's location.

4.2 Positioning tests

In section 2.4, the parameters required to compute the positioning algorithm were defined and explained. Among all the parameters, measurements computed by the receiver from satellite signals play a major role in the accuracy of the final position solution. As early mentioned in chapter 3, there are diverse signal configurations for each frequency band (see tables 3.1 and 3.2), and it is expected that each of them provide different position results. Due to this, it seems interesting to analyse them and try to extract some conclusions on the way. To do so, GPS L1-L5 and Galileo E1-E5 measurements will be read from an Observation RINEX together with its complementary Navigation RINEX.

The observation and navigation RINEX files used in this part, were downloaded from a reference station located in the province of Lleida in Catalonia, trhough *www.visorgnss.es* (see figure 4.4) and had a duration of approximately 4 hours (from 00:00h to $\approx$ 04:00). The reason to have selected this specific location is that it counted with a reasonable number of Galileo visible satellites and GPS's L5 signal measurements, which as it will be proved later, it is a not very common situation.

The metric to evaluate error in the position will be the cumulative distribution of the measured the 3D (X, Y, Z) root-mean-squared-error (RMSE from now on) in

meters, between the computed position and the real reference station position. The latter is contained in the Observation RINEX itself, as aforementioned in section 4.1. The cumulative distribution represents each error value together with its corresponding percentage in the entire experiment. Errors values which represent the 90% of the cases will be pointed out and selected as the metric to compare between different configuration.

4.2.1 GPS L1 - L5

It was mentioned in section 3.1, that at the reporting date, GPS does not count with enough L5 signals in its satellites so as to improve L1 navigation accuracy. As seen in figure 4.6, the maximum number of satellites with L5 signals during the whole observation period is of seven, whilst the minimum is of 4, which is the least allowed so as to be able to navigate (see section 2.4). For this, even though L5 signals are more modern and count with improved characteristics, the best option to navigate still is L1 band as they offer more signal redundancy to receivers. That the lack of L5 signals, not only impedes receivers to rely only on L5 band for positioning, but also prevents them from implementing rejection masks, e.g based in elevation or CN0 (see [42]), which tend to

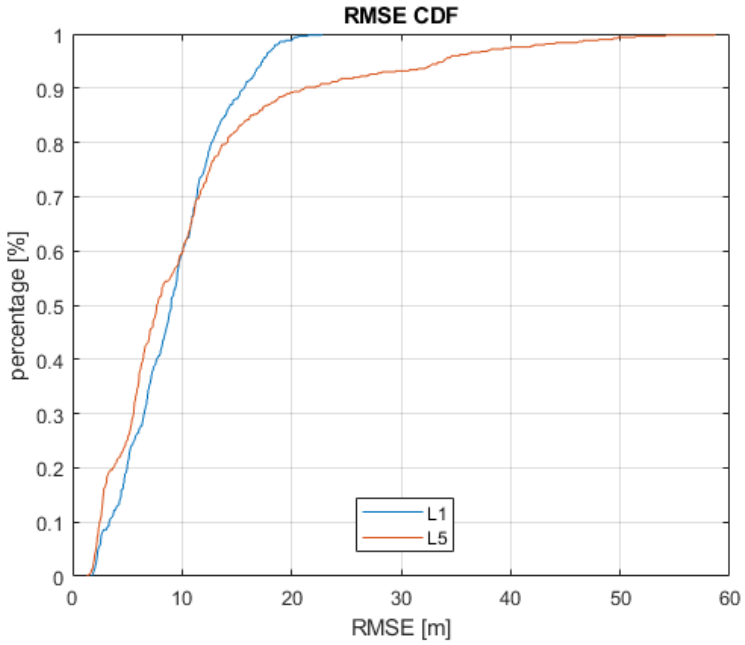

Figure 4.5: GPS L1 and L5 signals

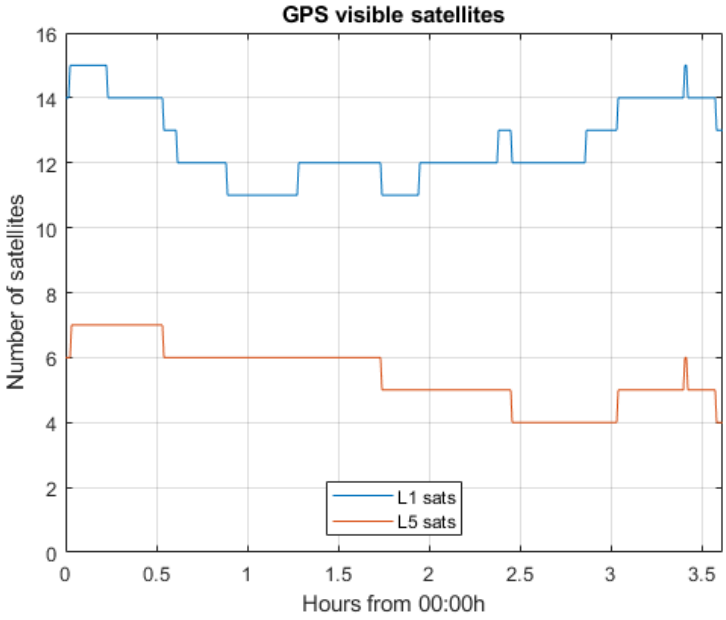

Figure 4.6: GPS satellites with L1 and L5 signals.

improve significantly positioning performances.
Results from figure 4.5 were obtained after testing L1 and L5 in the positioning algorithm. By relating the latter with figure 4.6, it is possible to determine that the greater L1 signal redundancy allow receivers to count with better satellite geometry and more representative position estimates, factors which are vital for a better positioning accuracy. On the other side, L5 signals' performance is not as bad as expected, as with only 4 to 6 satellite per epoch, it achieves a positioning accuracy not so far from L1 signals, which proves their potential in terms of accuracy. However, this RINEX was specially selected for counting with L5 measurements, that is, in other scenarios navigation using only L5 measurements is not advised.

4.2.2 GAL E1 - E5a

As explained in section 3.1 and in [26], E1 signals count with more modest specifications but with a larger bandwidth (BW) in comparison to E5a and E5b signals. In this specific case, E1 signals count with 32 MHz BW, which in the case of E5a signals it is of 27.795 MHz. By looking at figure 4.7 it is seen that Galileo's E1 position accuracy is slightly better than that from E5a ($\approx$ 0.67m). This points out that, in this specific scenario, a larger BW has contributed more to position accuracy than better signal specifications such as PRN code lengths, chipping rates etc.

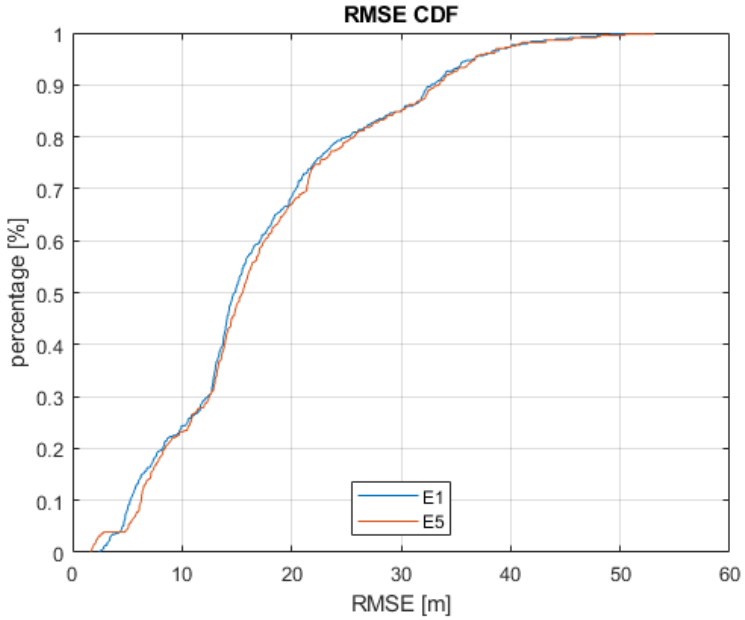

Figure 4.7: Galileo E1 and E5a signals.

In contrast to the case in the GPS constellation, all satellites count with Dual-Frequency measurements, that is E1 and E5 (see 4.10). For this, the resulting positioning accuracy in both bands is comparable. That being said, it is worth mentioning that the total number of visible satellites in average is still greater in the GPS constellation than in Galileo's, thus, signal redundancy and satellite geometry will be better in GPS.

4.2.3 E1 - E5b

In this specific case, Galileo E5b signal counts with a narrower BW than E5a. Concretely, E5b is transmitted in a 23.205 MHz BW, whilst E1 and E5a count with 32MHz and 27.795MHz BW. For this, after the results obtained in section 4.2.2 it is expected that its performance is worse than that from E5a. This fact is proved in figure 4.8, where E5b RMSE is the 90% of the cases $\approx$ 1.23 m greater than that from E1 signal.

4.2.3.1 E1 - E5ab

Even though E5a and E5b proved to perform similar to E1 in this specific scenario, Galileo offers the possibility of combining E5a and E5b in such a way which increases dramatically the resulting signal BW. This combination provides a 40MHz BW, which in contrast to E1 signals BW is 8 MHz wider. To perform this comparison, mobile phone GNSS data

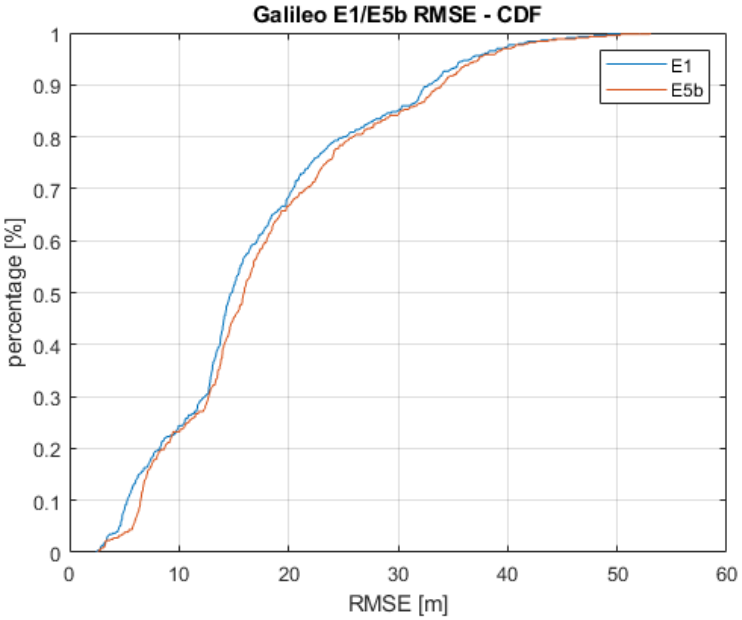

Figure 4.8: Galileo E1 and E5b signals.

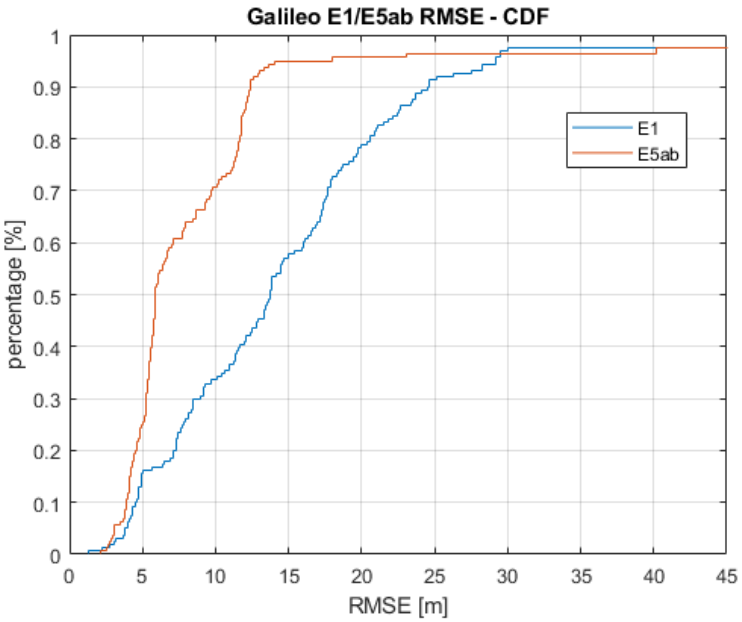

Figure 4.9: Galileo E1 and E5ab signals.

was used. The obtained results are displayed in figure 4.9. It is possible to see that there is substantial improvement in E5 signals performance over E1 signals when the full E5 BW is used. As mentioned in 3.1, when E5a and E5b are combined to form E5 full band, the resulting modulation provides better specs in terms of error probability 3.4 for a given Carrier-to-Noise ratio (CN0) (see [43]).

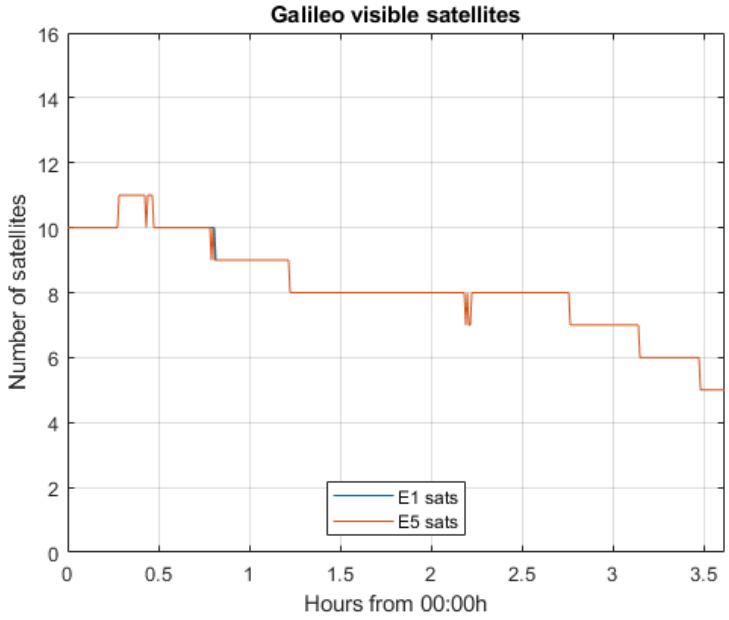

Figure 4.10: Galileo satellites with E1 and E5 signals

4.3 Ionosphere corrections for SF receivers

It was noted in 3.3.2 that when satellites do not provide DF measurements, the only way of obtaining corrections to mitigate ionosphere delay is by using the so-called broadcast models. This is the case of GPS in particular, which currently lacks in L5 signal measurements. In the case of Galileo, all satellites count with DF measurements, and thus, broadcast models are mostly reserved for those receivers limited to work with one frequency band (usually E1), and for certain scenarios that later will be mentioned. For this, the following error mitigation techniques regarding broadcast models and their combination with DF measurements will be focused in the GPS system, as the corrections obtained in the Galileo constellation from DF measurements are effective enough.
Section 3.3.2 also pointed out that it is expected that Necquick-G performs better than Klobuchar, but also requires more computational capabilities and it is not as simple. For simplicity, we will work with the Klobuchar model and see its effects in position results.

In section 4.2, the positioning algorithm was implemented for both GPS and Galileo L1 and L5 frequency bands. In this case, it is desired to perform the very same positioning algorithm including Klobuchar model's ionosphere delay correction. In order to do so, the value returned by the function which performs Klobuchar will be substracted from

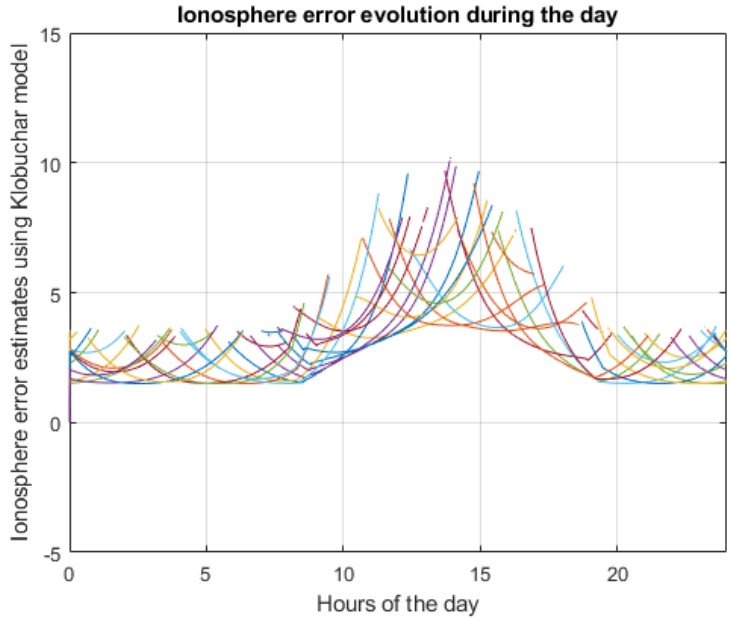

Figure 4.11: Klobuchar's Ionosphere error estimates during a whole day (from 00:00h to 23:59h).

pseudorange measurements. In this case, the process would be as simple as:

$$\rho_{IF}^{(k)} = \rho^{(k)} - \hat{I}_{K}^{(k)}$$

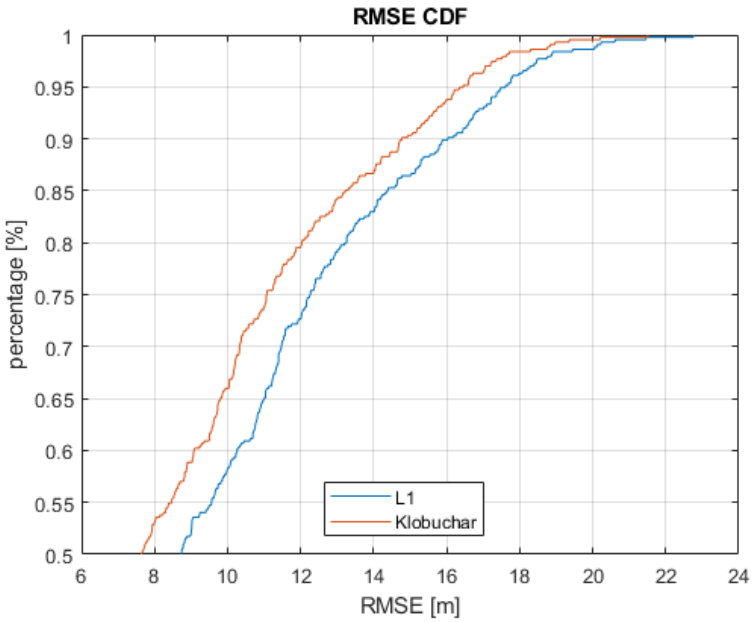

Figure 4.12: GPS PVT RMSE CDF - Klobuchar

In figure 4.11 it is possible to see Klobuchar model estimates obtained from a RINEX file containing 24 hours of observables. From this figure it is important to notice that estimates follow deterministic traces and that that their noise contribution will be minimal.
When these estimates are applied to the positioning algorithm, results of figure 4.12 are obtained. In this figure it is seen that by applying these corrections, the resulting RMSE error is reduced a approximatelly 1.5 meters in the 90% of the cases.
In result, it can be concluded that although Klobuchar correction may not substract all ionosphere delay from measurements, it is very consistent, as it can be applied to all signal measurements. This will be seen in more detail when compared with other correction techniques.

4.4 Ionosphere corrections for DF receivers

DF compatible receivers are capable of either using broadcast model ionosphere delay corrections and computing their own estimates based on DF measurements.
Figure 3.7 displays DF ionosphere error estimates obtained from using espression 3.6 from a RINEX file contianing 24 hours of observables. Ionosphere error estimates from figure 3.7 were obtained using expression 3.6, with the same 24 hours RINEX file used

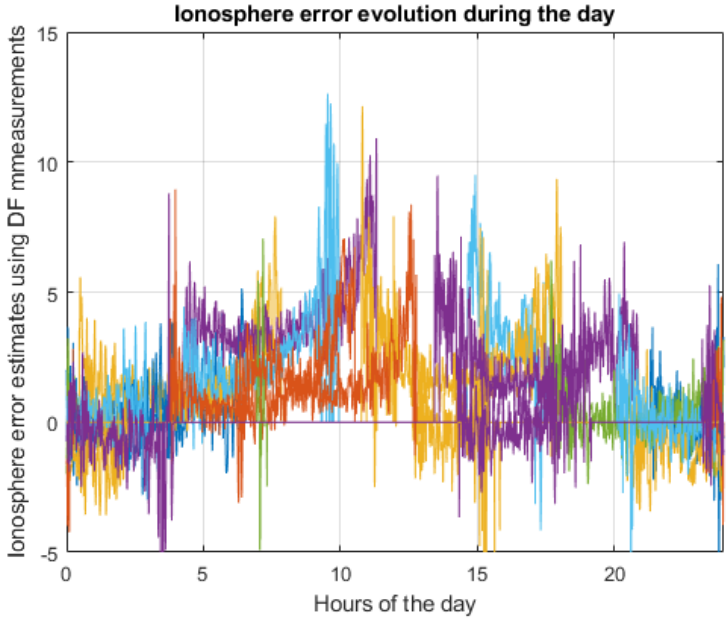

Figure 4.13: GPS DF Ionosphere error estimates during a whole day (from 00:00h to 23:59h).

in the past section.
In this figure it is possible to see that the resulting estimates are dramatically noisy, specially when compared to those from the Klobuchar model. In addition, one can see certain values below the zero threshold which are physically impossible, that is, negative errors of the Ionosphere correction would mean that the corresponding pseudorange measurements are in fact shorter. This, at the same time would mean that the ionosphere layer increased the signal's velocity, which is the speed of light, and that is plainly impossible. These erroneous values come from the fact that, in the expression which estimates the ionosphere error, the combinations of both pseudorange are so noisy that result in a wrong measurement.
It is also noticeable, that the maximum Ionosphere correction observed is not exactly at 14:00h as in the Klobuchar model but around 12:30 and 13:30. These values are more deterministic an represent better the actual ionosphere state.
As mentioned earlier, Galileo is able to obtain DF corrections for all its signal measurements. In contrast, GPS will only be able to correct from 4 to 6 signal measurements (see figure 4.6). For this, the impact of applying DF corrections in the case of Galileo is expected to be much more positive than in GPS.

Results obtained after applying this DF corrections in GPS and Galileo constellaitons are displayed in figures 4.14 and 4.15, respectively. By looking at figure 4.14, it is

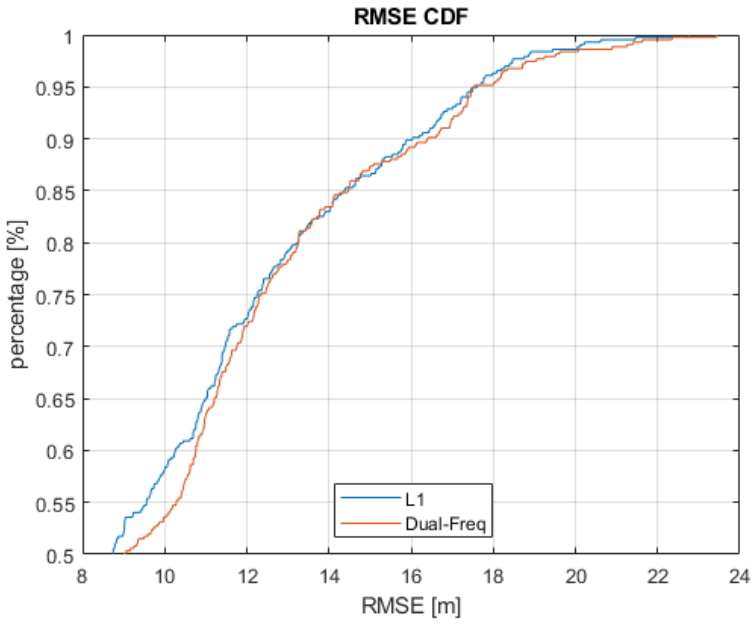

Figure 4.14: GPS PVT RMSE CDF - DF

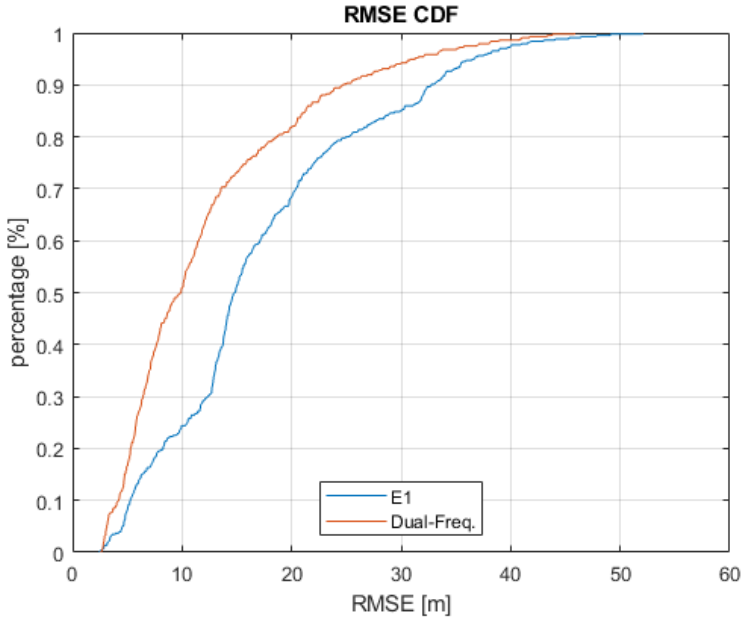

Figure 4.15: GAL PVT RMSE CDF - DF

clear that the noise contribution of DF corrections are affecting negatively the positioning accuracy. It can be determined that the amount of error introduced to measurements is greater than the correction factor. However, in the case of the Galileo constelation, DF corrections improve greatly the positioning accuracy, as all satellite measurements used in the PVT algorithm have been corrected.
In the case of GPS, it can be concluded that applying few raw DF measurements is only advisable when little signal processing capabilities are available in the receiver and the ionosphere effects are greater in measure than the amount of error which will be introduced to the system. As the RINEX file used comes from a reference station located in Lleida (Catalonia), which is considerably far from the Earth's equator, it is expected that the ionosphere error contribution is not significant enough to justify applying raw DF measurements.

4.4.1 Combining Ionosphere error estimates.

This section aims to improve the correction factor obtained in GPS when applying Klobuchar and DF measurements corrections separately, by combining them. On the one hand, it was noted in section 3.6, that DF measurements estimate ionosphere errors with a $\approx 99\%$ of accuracy, whilst Klobuchar at $\approx 50\%$. On the other hand, Klobuchar model provides a greater amount of corrections than DF meaurements in GPS. For this,

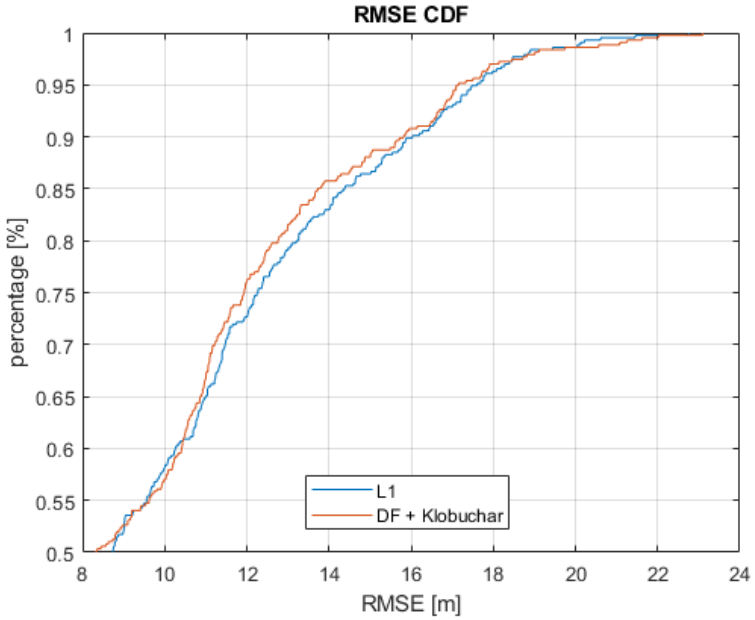

Figure 4.16: GPS PVT RMSE CDF - Klobuchar & DF correction

DF receivers tend to combine these measurements, that is, available DF corrections are prioritised over the Klobuchar model corrections, which are applied to SF measurements. The corresponding results are displayed in figure 4.16, where it is possible to see a slight improvement over applying only DF corrections. However, the noise from DF measurements make the total correction factor to be worse than only applying Klobuchar.

4.4.2 Improving DF measurements.

The aim of this section is to look for techniques which improve the quality of DF measurements so as to improve results obtained so far. For this, we will try to mitigate one of the main cons of DF measurements, which are its noisy nature. To do so, we will make use of carrier phase measurements contained in RINEX files.

Carrier phase measurements are not as often used for positioning, as they are a priori ambiguous. To substract amguities from phase measurements, receivers need to analyse and track their changes between epochs, which delays the positioning process and adds more computational burden (see [8] (ch.7) for more information). Despite of this, receivers are able to obtain much more precise measures from the signal's carrier phase rather than from its code. In consequence, it is desired combine these ambiguous but precise carrier phase measurements with the non-ambiguous but noisy code measurements. The key factor that relates both measurements are their change between consecutive time

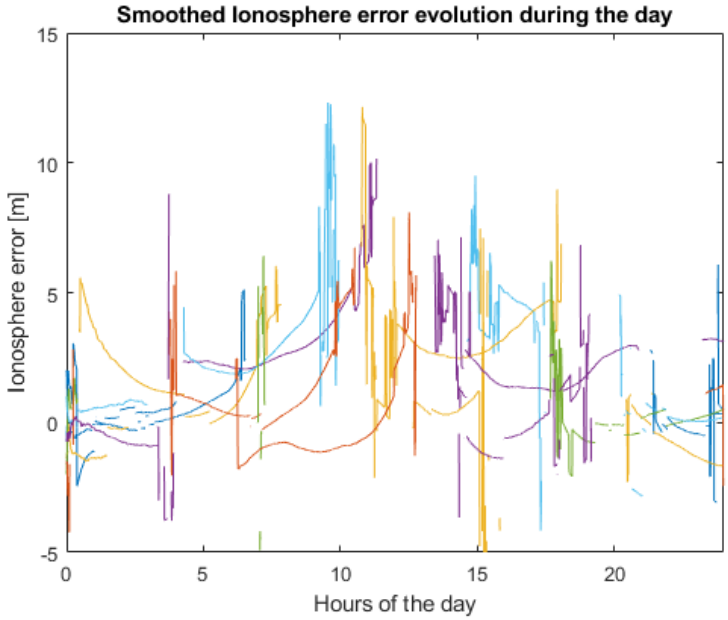

Figure 4.17: DF Smoothed Ionosphere error estimates during a whole day (from 00:00h to 23:59h).

epochs. That is, the change between two carrier phase measurements should be the same that in code measurements. However, this change is determined with much more accuracy in using signal's carrier phase. For this, an initial state could be taken from code measurements, and from then on its evolution could be propagated with phase measurements. However, this technique has to take a major consideration into account, and its related to the receiver's capability to keep track of satellite measurements. In the case a satellite became non-visible for the receiver, or the receiver lost its tack, the resulting change in carrier phase measurements would not reflect the change between code measurements as carrier phase ambiguities would have changed. For this, in such cases the propagation algorithm should reset and start again with another initial code measurement.

This algorithm commonly used to perform this technique is the so-called Hatch filter, which is explained in much more detail in [44]. The basic formal expression of this filter, is the following:

$$\begin{aligned} \hat{\rho}(s;k) &= \frac{1}{n}\rho(s;k) + \frac{n-1}{n}[\hat{\rho}(s;k-1) + (\phi(s;k) + \phi(s;k-1))], \\ where \quad (n=k) \quad if \quad (k<N) \quad and \quad (n=N) \quad when \quad (k \bar{>} N). \end{aligned} \tag{4.1}$$

Where ρ and ϕ are the code and carrier measurements of a satellite s at time n, and $\hat{\rho}$ is the smoothed code measurement.

The resulting smoothed ionosphere error is displayed for a whole day in figure 4.17, and its compared to the previous noisy ionosphere error for GPS PRN 1 and PRN 8 in figure 4.19. These estimates will be applied to measurements combined with Klobuchar estimates as in the previous test.
Figure 4.18 clearly shows that results obtained are not very different than before, when no smoothed was performed. From this result one can deduce that the problem in the noisy ionosphere error estimates is not their variance. In fact, it is the variance of code measurements from which they we obtained, that bias the resulting estimates. For this, even if these are smoothed, they will still be biased and provide a wrong correction factor.

To mitigate this bias, the Hatch filter should be applied before obtaining any Ionosphere estimate. For this, we can think of smoothing pseudorange differences from expression 3.6, so that the resulting estimates are less biased. To do so, it is also needed to compute carrier phase measurement differences so as to propagate code differences in time.
From expression 3.6,

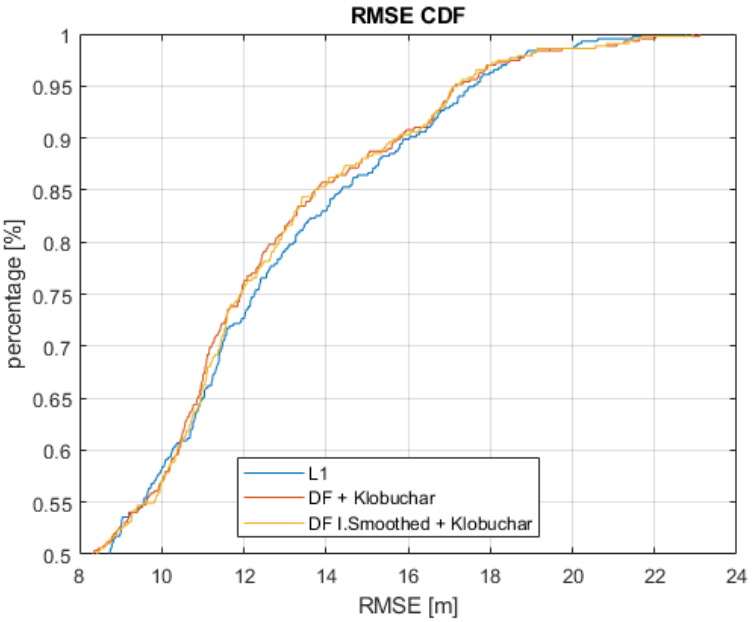

Figure 4.18: GPS PVT RMSE CDF - Klobuchar & DF. Iono. Smoothed correction.

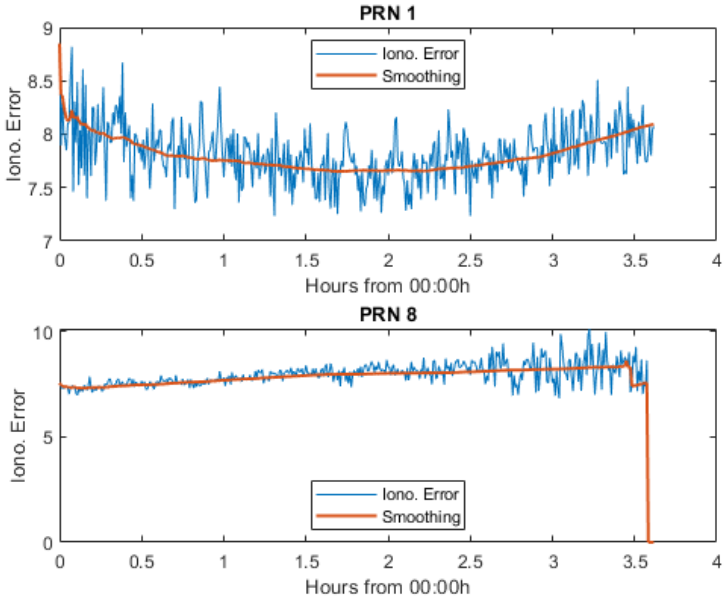

Figure 4.19: Smoothed DF Ionosphere error estimates for PRN 1 & PRN 8.

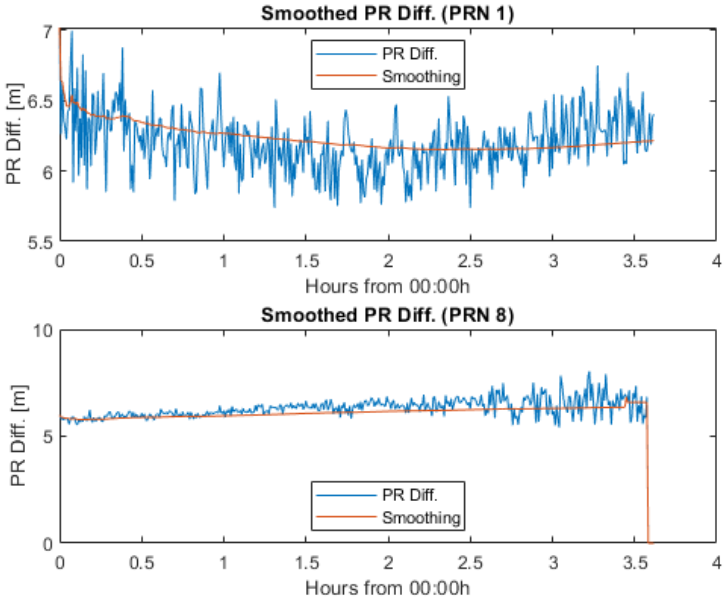

Figure 4.20: Smoothed PR. Diff for PRN 1 & PRN 8.

$$\hat{I}(f_i) = \frac{A}{f_i} = (\rho_{(j)} - \rho_{(i)}) \cdot \frac{f_j^2}{f_i^2 + f_j^2}$$

A new variable is defined:

$$\Delta\rho = (\rho_{(j)} - \rho_{(i)})$$

and equivalently, for phase measurements:

$$\Delta\phi = (\phi_{(j)} - \phi_{(i)})$$

Finally, these new variables are included to the Hatch filter, such as:

$$\Delta\hat{\rho}(s;k) = \frac{1}{n}\Delta\rho(s;k) + \frac{n-1}{n}[\Delta\hat{\rho}(s;k-1) + (\Delta\phi(s;k) + \Delta\phi(s;k-1))]$$

The resulting estimates not only will contain less noise, but also will be less biased. It is noticeable by comparing figures 4.19 and 4.20 that both the smoothed ionosphere error and the smoothed difference between range measurements have different tendencies. The resulting ionosphere estimates from both cases are compared in figure 4.21, where it is clear that their correction factor will be different.
That being said, by looking at figure 4.22 it is proved that that when these estimates are applied to measurements, their impact in position accuracy is more notorious and positive than in the previous case.

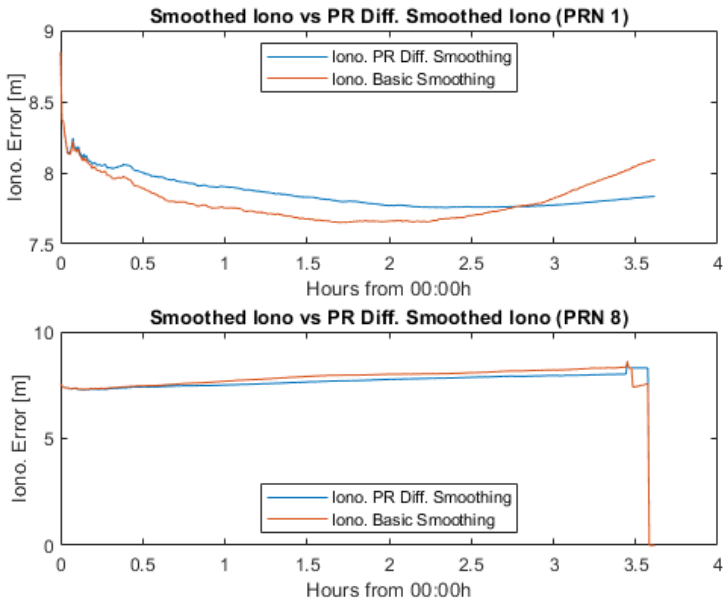

Figure 4.21: Smoothed Iono. Error vs Iono. Error (PR Diff. Smoothed)

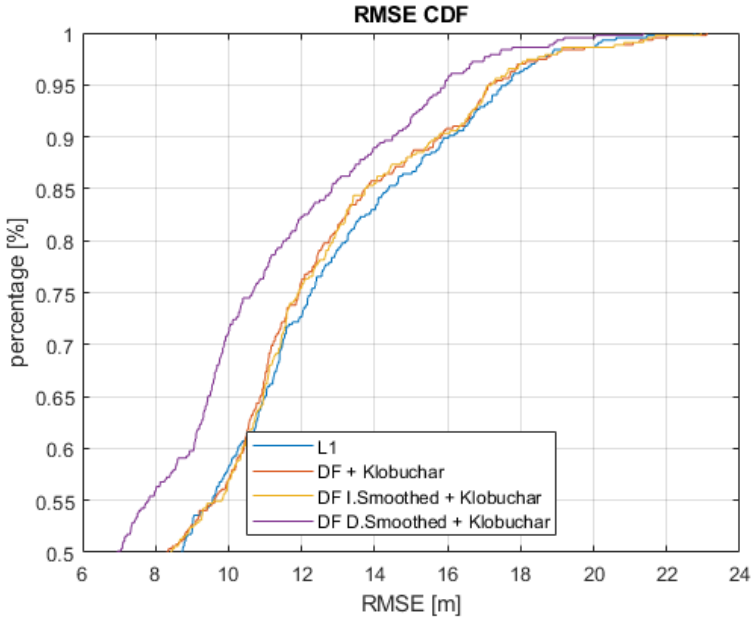

Figure 4.22: GPS PVT RMSE CDF - Klobuchar & DF. Diff.Smoothed correction

4.4.3 Combining Ionosphere-free measurements

Until this point, all techniques were based in correcting L1 band measurements to later use them in the positioning algorithm. With the aim of improving position accuracy, we could think of including both L1 and L5 signal measures. However, if the frequency-dependent error component, which is the ionosphere error, is removed, the resulting corrected estimates would theoretically be equal in either L1 and L5 bands. For this, the effect of including them both in the PVT algorithm would be to weight favourably DF measurements (by a factor of 2), assuming all satellites with L5 signals also count with L1 signals (which is the common case). This would mean that the PVT algorithm would 'trust' more measures which have had ionosphere errors striped off by means of DF corrections. That being said, in this section both L1 and L5 will first corrected in their respective frequency bands, by means of the aforementioned difference-smoothed ionosphere error estimates, and later included in the PVT algorithm and see their effect in positioning. The process followed is derived from expression 4.2, as:

$$\Delta x = (H^T H)^{-1} H^T \Delta\rho \tag{4.2}$$

where,

$$H = \begin{bmatrix} e_{x\,L1}^{(1)} & e_{y\,L1}^{(1)} & e_{z\,L1}^{(1)} & 1 \\ \vdots & \vdots & \vdots & \vdots \\ e_{x\,L1}^{(Nsat)} & e_{y\,L1}^{(Nsat)} & e_{z\,L1}^{(Nsat)} & 1 \\ e_{x\;\;L5}^{IF(k)} & e_{y\;\;L5}^{IF(k)} & e_{z\;\;L5}^{IF(k)} & 1 \\ \vdots & \vdots & \vdots & \vdots \\ e_{x\;\;L5}^{IF(K)} & e_{y\;\;L5}^{IF(K)} & e_{z\;\;L5}^{IF(K)} & 1 \end{bmatrix} \tag{4.3}$$

$$\Delta\rho = \left[\Delta\rho_{L1}^{(1)}, \quad \ldots, \quad \Delta\rho_{L1}^{(k)}, \quad \Delta\rho_{L5}^{IF(1)}, \quad \ldots, \quad \Delta\rho_{L5}^{IF(k)}\right] \tag{4.4}$$

Where:

e accounts for the unitary satellite to receiver line-of-sight vector from eq. 2.4 and the subscript k makes reference to the L5 measurements subset from the total set of L1 satellites.

It is noticeable that all L5 measurements contain the subscript ρ^{IF} as all of them have been corrected using DF measurements, (again, it is assumed there are always L1

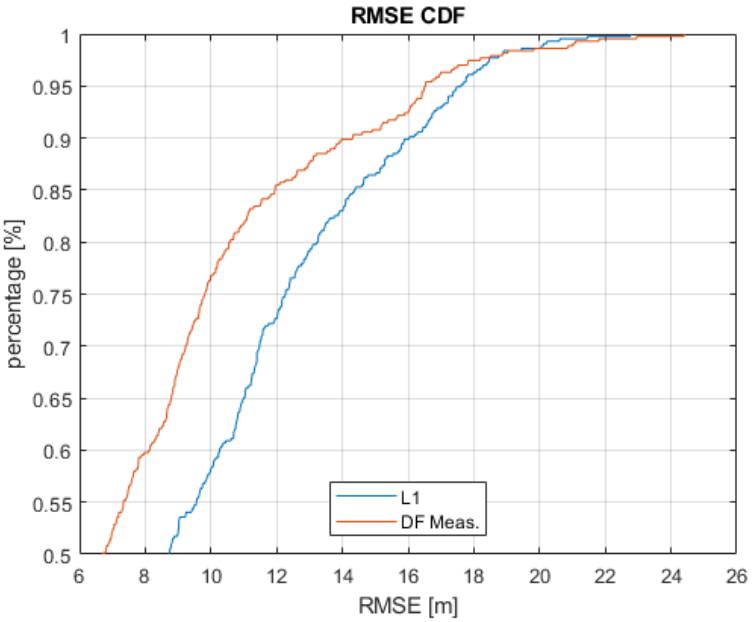

Figure 4.23: GPS PVT RMSE CDF - Klobuchar & DF L1-L5 Diff. Smoothed corrections

measurements for any given PRN).

The obtained results are displayed in figure 4.23, where it is possible to see a slight improvement over the previous correction technique in the 90% of the cases.
The performance of this technique depends on the conditions of the satellite constellation and the scenario in which it is applied. If satellites with DF signals counted with bad measurements, or low CN0 levels, maybe the effect of weighting them more than the rest of satellites would be more negative than positive overall. For this, it is believed that this technique has the potential to improve if more considerations are taken into account to make it more robust to these error sources.
All correction techniques results have been gathered in figure 4.24 and in table 4.1 for comparison purposes.

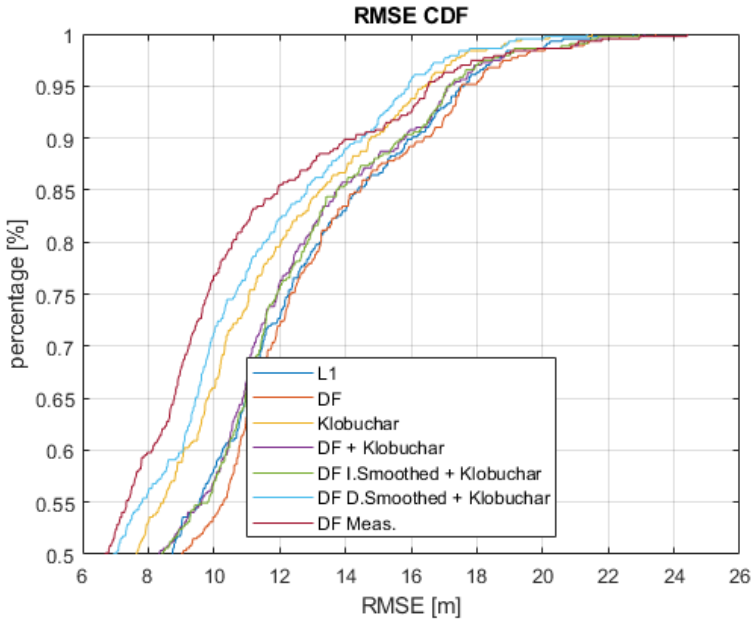

Figure 4.24: GPS PVT RMSE CDF - All corrections compared

GPS	RMSE [m] (90%)	**Correction [m]**
L1	16.03	-
L1 + Klobuchar	14.77	**1.26**
L1 + DF	16.4	**-1.37**
Klob. + DF	15.79	**0.24**
Klob. + DF Iono. Smoothed	15.74	**0.29**
Klob. + DF Diff. Smoothed	14.49	**1.54**
Klob. + DF L1-L5	14.31	**1.72**

Table 4.1: All tests compared

Chapter 5

Conclusions

This chapter is targeted at reminding the initial purposes which motivated this research and to evaluate the conclusions extracted from the analysed results.

As it was mentioned in the introduction, this thesis had two major goals. The first one was addressed in chapter 2. Its aim was to introduce GNSSs and to explain the basic positioning principles, in the most comprehensive and understandable way.
The second one was handled in chapter 3, and put special interest in explaining the evolution of GNSS signals and in particular the use of Dual-Frequency measurements for positioning. In order to cover these objectives, the research was divided in two parts, and for the sake of simplicity, conclusions will be organised in the same way.

The conclusion of the first part is that it has been satisfactorily achieved. Chapter 2 has provided the background and basic equations of GNSS required to later understand the concepts of chapter 3 and to perform the tests from chapter 4.

As for the conclusions from the second part, these will be pointed out in different sections to present them more clearly.

5.1 Dual Frequency measurements

GPS and Galileo signals from both L1/E1 and L5/E5 bands where introduced in section 3.1. In the latter it is mentioned that the availability of L5/E5 signals not only provides

receivers with an alternative to the historical L1 frequency band to navigate, but also allow them to combine its measurements so as to improve positioning accuracy. However, the impact of these signals in navigation depends on several aspect which will be pointed out next.

In the case of Galileo, E5a and E5b signals count with better specifications than E1, which is the most frequently used for common receivers. E1 signal on its side, is transmitted using a wider BW than the others. Greater BW is related to higher processing gains [34] in spread spectrum systems. Either a greater BW and better signal specifications will allow receivers to obtain more accurate estimates.
Results from figures 4.7 and 4.8 suggest that the increase in E1 signal BW outperforms better signal specs, as it provides slightly better positioning results. The worse case in this scenario the one with narrower BW, that is E5b signal.
This hypothesis is finally proved when mobile phone GNSS data is used to compute the position using the full E5 signal, which combines the spectrum from both E5a and E5b signals. In this scenario, the E1 signal offered a position accuracy of 24.43 meters whilst E5ab managed to reduce this error with respect the actual position down to 12.2 m. This measurements are displayed in table 5.1. That being said, it can be concluded that receivers which do not meet the requirements to cope with the full E5 signal, should count in E1 signal as the alternative to navigate.

The case of GPS is way different than that from Galileo. In this context, although L5 signals also improve L1 specifications, navigation using only L5 signal measurements is directly not advised. The lack of satellites transmitting in the L5 band degrade the system performance in terms of satellite geometry and measurements redundancy, and in certain time epochs imposes the receiver to use all visible to solve for its position.

GAL	RMSE [m] (90%)	BW [MHz]
E1	32.6	32
E5a	33.43	27.795
E5b	33.99	23.205
E5ab (E1 = 24.43 m)	12.2	40

Table 5.1: Galileo signals PVT performances

This fact prevents receivers from implementing hardly any rejection masks, which tend to improve considerably positioning accuracy. Besides as less amount of DF corrections can be applied, receivers need to rely more on broadcast models and signal processing techniques to subtract ionosphere errors from its measurements.
The main advantage of the GPS constellation is that it offers a greater total number of visible satellites transmitting in the L1 band. For this, it outperforms Galileo's availability, measurement redundancy and satellite Geometry.

5.2 Ionosphere error mitigation

It has been seen that two approaches are considered to correct ionosphere errors in signal measurements. The first one is to make use of broadcast models, such as GPS's Klobuchar, to obtain ionosphere error correction estimates. The second one is to compute these estimates by combining DF measurements.

In the Galileo GNSS, all satellites count with DF measurements (see 4.10). Thus, all signals can be corrected using DF estimates. In result, the final correction factor mitigates substantially ionosphere errors, as it is proved in figure 4.15.

As for the GPS GNSS, the situation is very different. Only a small subset from the total amount of visible satellites per time epoch counts with DF measurements. For this, fewer DF corrections will be applied, which at the same time will reduce considerably the final correction factor in the computed position. In fact, figure 4.14 demonstrates that the correction factor is smaller than the error introduced by DF corrections in measurements. For this, the obtained position is worse than the one without any corrections applied. In conclusion, the use of DF corrections alone is not advised in the GPS constellation to avoid positioning errors.
An alternative would be to apply Klobuchar corrections to all satellites. With this, results from figure 4.12 were obtained, where the position accuracy was improved considerably. However, it is desired to make use of avialiable DF measurements in such a way that outperforms the correction factor Klobuchar alone. With this aim, various correction techniques were tested, which for the sake of simplicity are gathered in a set of bullet-points:

- **Combining Klobuchar & DF:**
  This combination aimed to solve the lack of DF satellites. For this, Klobuchar estimates were applied to those satellites which do not count with DF measurements. Results from figure 4.16 prove that, even though position accuracy is slightly improved, the total correction factor provided by the Klobuchar model alone is still greater.

- **Combining Klobuchar & DF (Iono.Smoothed):**
  This technique aimed to reduce the noise component from DF corrections so as to obtain better correction estimates. For this, the Hatch filter was introduced and applied to ionosphere error estimates (see 4.19). As seen in figure 4.18, results seemed to not improve much with respect to only combine DF with Klobuchar. This fact came from the fact that ionosphere error estimates where previously biased by the noisy pseudorange combination from expression 3.6.

- **Combining Klobuchar & DF (PR Diff.Smoothed):**
  With the aim of reducing the bias introduced in ionosphere correction estimates, the hatch filter was applied before they were obtained. That is, pseudorange differences where smoothed using carrier phase differences, which were less noisy 4.20. In this case, results obtained improved previous correction factors 4.22. With this result it is determined that in order to increase the correction factor of few GPS DF measurements combined with the Klobuchar model with respect to the noise introduced, proper non-biased smoothed estimates are required.

- **Combining L1 and L5 DF measurements:**
  In this technique the positioning algorithm was slightly modified to include both L1 and L5 ionosphere-free signal measurements. In the case errors had been mitigated properly, either L1 and L5 would provide the same measurements and thus, would double their weight in the positioning solution. Results obtained from this technique were also positive and slightly better than the previous case in the 90% of the cases (see figure 4.24) for the selected scenario. However, if ionosphere errors were not compensated effectively, both L1 and L5 signals would not improve satellite redundancy, but would include more error in the solution. In addition, it is worth mentioning that including L1 and L5 measurements in the LS does not affect positively satellite geometry, as their corresponding LoS vectors would be linearly dependent.

In conclusion, receivers should take the following considerations into account before using

DF measurements to correct ionosphere effects:

- In the case of GPS, which counts with few DF measurements, raw DF corrections should only be applied in very harsh scenarios where ionosphere effects are strong, and the correction factor provided will be greater than the error introduced in measurements. This is proved in figure 5.1, where it is possible to see that position solutions which have been corrected with biased ionosphere error estimates and count with lower correction factor, increase the RMSE error in certain epochs.
- Due to the noisy nature of range measurements, they should be first smoothed or averaged before used to estimate ionosphere corrections. With this, the resulting estimates will be less biased and more representative of the actual ionosphere error in measurements.

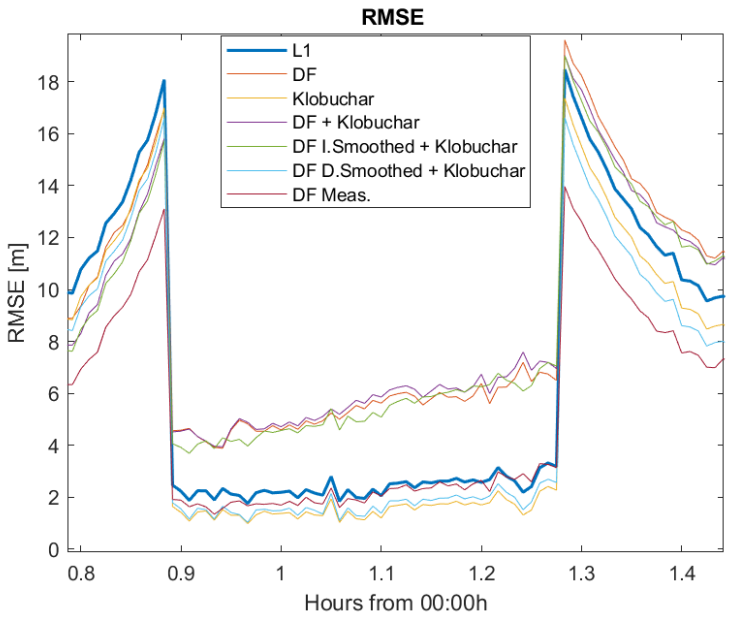

Figure 5.1: GPS PVT RMSE - Effect of non-smoothed corrections

5.3 Future lines of research

Thanks to the increasing signal redundancy in the GPS constellation and the nearly completed Galileo's satellite fleet, new lines of research arise to determine the best signal configurations and correction techniques for future applications requiring navigation services, according to their necessities. The most relevant requirements for future applications have been gathered below:

- **Integrity for safety critical applications:**
  In certain applications of safety-of-life, such as aircraft guidance, integrity constitutes one of the most demanded requirements, as a constant high level of position accuracy is necessary. In this context, a major threat for these applications are ionosphere effects, as they constitute of a considerable error source whose behaviour depends upon many factors, such as user location, local time, season of year and solar activity (see section 3.3.1). According to [2], ionosphere errors are not corrected enough by current GNSS core constellation techniques such as the aforementioned in section 4.4. For this, satellite based augmentation systems (SBAS) are being used to provide position information including more accurate ionosphere corrections to meet integrity requirements for the intended operations. However, once all L5 signals are added to GPS satellites and Galileo is fully operational, more signal combinations and error mitigation techniques could be tested with the aim of reducing the system dependency on SBAS corrections to meet integrity necessities.

- **Cost-effective solutions:**
  There are other applications whose requirements are way different than those from safety-of-life. For example, in mass-market devices, the current necessities are low resource-demanding navigation techniques, which keep positioning errors under a considerable threshold when used in receivers with limited capabilities (see [45]). For this, research based on new signal configurations which meet these requirements at the minimum cost could be done. Different signals and ionosphere error corrections techniques could be combined and tested not only increase or maintain position accuracy but also to reduce the computational cost.

Bibliography

[1] Rui Barradas Pereira. GNSS applications. *Navipedia*, 2011.

[2] INTERNATIONAL CIVIL AVIATION ORGANIZATION ASIA and PACIFIC OFFICE. SBAS safety assessment guidance related to anomalous ionospheric conditions. 2016.

[3] Navigation National Coordination Office for Space-Based Positioning and Timing. GPS modernisation plan. *GPS.gov*, 2017.

[4] GMV. Galileo future and evolution. *Navipedia*, 2011.

[5] Frank van Diggelen and Mohammed Khider. GNSS analysis tools from google. *InsideGNSS*, 2018.

[6] ESA. Galileo App competition, 2018.

[7] Kegen Yu, Ian Sharp, and Y. Jay Guo. Hyperbolic navigation. *ResearchGate*, 2009.

[8] P. Misra and P. Enge. *Signal Measurements and performance*. Ganga-Jamuna Press, 2006.

[9] Ben A. Witvliet and Rosa Ma Alsina-Pagès. Radio communication via near vertical incidence skywave propagation. *Springer US*, 2017.

[10] Wikipedia. Sputnik 1, 2019.

[11] R. Píriz, B. Martín-Peiró, and M. Romay-Merino. The galileo constellation design: A systematic approach. *ION GNSS 2005*, 2005.

[12] Chen Jianyu. Overview of compass/beidou navigation satellite system. *ION Newsletter*, 2007.

[13] GMV. Galileo ground segment.

[14] B.W. Parkinson and S.W. Gilbert. Navstar: Global positioning system – ten years later. *Proc. IEEE 71(10)*, 1983.

[15] Liu C.J. Effects of selective availability on gps positioning accuracy. *Southern Journal of Applied Forestry*, 2002.

[16] V.V. Dvorkin, Y.I. Nosenko, Y.M. Urlichich, and A.M. Finkel'shtein. The russian global navigation satellite program. *Her. Russ. Acad.*, 2009.

[17] J.S. Lee and L.E. Miller. Cdma systems engineering handbook. *Artech House*, 1998.

[18] Wikipedia. Direct-sequence spread spectrum, 2019.

[19] R. Gold. Optimal binary sequences for spread spectrum multiplexing. *IEEE Trans. Inf. Theory.*

[20] James A. Slater and Stephen Malys. *WGS 84 — Past, Present and Future.* Springer, 1998.

[21] UPC. Reference systems and frames, 2011.

[22] G. Beutler. *Methods of Celestial Mechanics.* Springer, 2005.

[23] Teunissen and Montenbruck. *Springer Handbook of Global Navigation Satellite Systems.* Springer, 2017.

[24] InsideGNSS. Assessing GNSS data message performance. *InsideGNSS*, 2013.

[25] U.S. GPS. IS-GPS-200, 2018.

[26] European GSA. Galileo OS signal-in-space ICD, 2016.

[27] J.R. Vetter. Fifty years of orbit determination: Development of modern astrodynamic methods. *Johns Hopkins APL Tech.*, 2007.

[28] E. Kaplan & J. Hegarty. *Understanding GPS.* Artech House, 2006.

[29] Steven J. Miller. The method of least squares. *Brown University*, 2012.

[30] European Commission. Ionospheric correction algorithm for galileo single frequency users. 2016.

[31] U.S. Goverment. Global positioning system standard positioning service performance standard. 2008.

[32] U.S. GPS. IS-GPS-705, 2018.

[33] J.A Ávila Rodríguez. GPS signal plan. *Navipedia*, 2011.

[34] John Fakatselis. Processing gain in spread spectrum signals. *Harris Semiconductor*, 2011.

[35] J.A Ávila Rodríguez. Galileo signal plan. *Navipedia*, 2011.

[36] Cecile Deprez. Relative positioning with galileo E5 AltBOC code measurements. *ResearchGate*, 2016.

[37] Cyril Botteron Pierre-André Farine Miguel Angel Ribot. Derivation of the cramér-rao bound in the gnss-reflectometry context for static, ground-based receivers in scenarios with coherent reflection. *École Polythecnique Fédérale de Lausanne*, 2016.

[38] Frank Nielsen. Cramer-rao lower bound and information geometry. *École Polythecnique*, 2013.

[39] J. Sanz Subirana, J.M. Juan Zornoza, and M. Hernández-Pajares. Klobuchar ionospheric model. *Navipedia,*, 2011.

[40] Oliver Julien, Jean-Luc Issler, Laurent Lestarquit, and Lionel Ries. Estimating ionospheric delay. *InsideGNSS*, 2015.

[41] Receiver independent exchange format, 2018.

[42] A GNSS Satellite Selection Method Based on SNR Fluctuation in Multipath Environments. Yuan ya fang and yuan hong2 and ouyang guang zhou and wang liang and and liu wenxue. *University of Chinese Academy of Sciences*, 2015.

[43] Robert Kieser, Pall Reynisson, and Timothy J. Mulligan. Definition of signal-to-noise ratio and its critical role in split-beam measurements. *ICES Journal of Marine Science,*, 2005.

[44] Hatch & Ron. The synergism of GPS code and carrier measurements. 1998.

[45] University of texas. Precise positioning for the mass market. 2016.

[46] Daniel Egea, Jose A. Lopez Salcedo, Gonzalo Seco Granados, and Jean-Marie Sleewaegen. GNSS measurement exclusion and weighting with dual polarized antenna: The FANTASTIC project. *ResearchGate*, 2018.

[47] Gonzalo Seco Granados, José A. Lopez Salcedo, David Jiménez Baños, and Gustavo López-Risueño. Challenges in indoor global navigation satellite systems. *IEEE Signal Processing Magazine*, 2012.